UCSB

Widely Tunable MetaResonators for Reconfigurable Infrared Metasurfaces

Prof. Jon A. Schuller
Electrical and Computer Engineering Department
UC Santa Barbara

Meta-Optics and Metamaterials Workshop
Center for Theoretical Physics of Complex Systems
April 23, 2018

---------------Funding--------------

AFOSR
AIR FORCE OFFICE OF SCIENTIFIC RESEARCH

Northrop Grumman

Programmable Optics & Metasurfaces

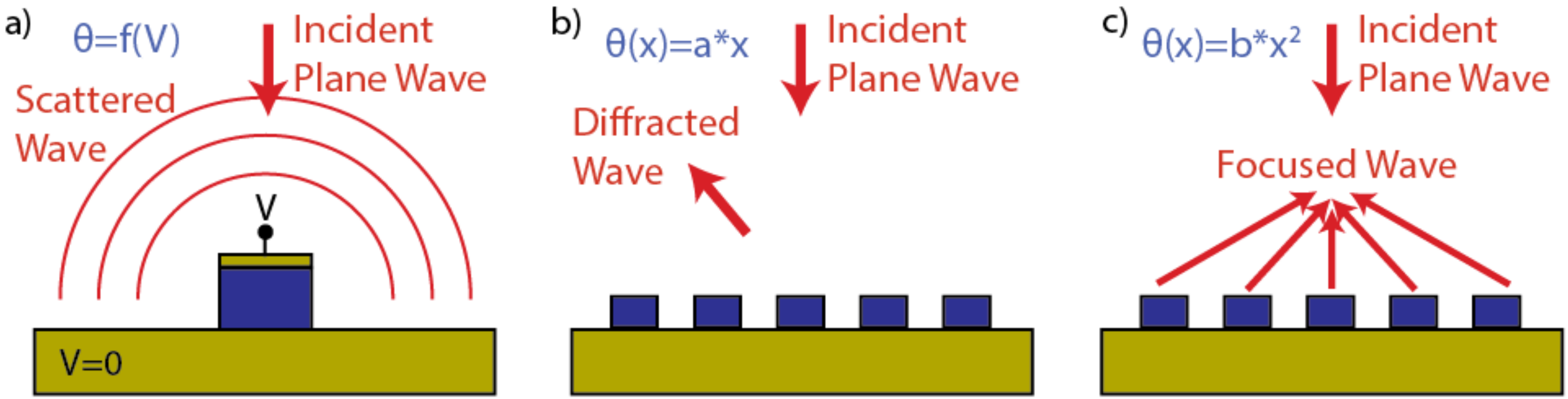

- **Goal: Continuous tuning between 0 and 2π with minimal change in amplitude**

Mie Resonators: Experiments

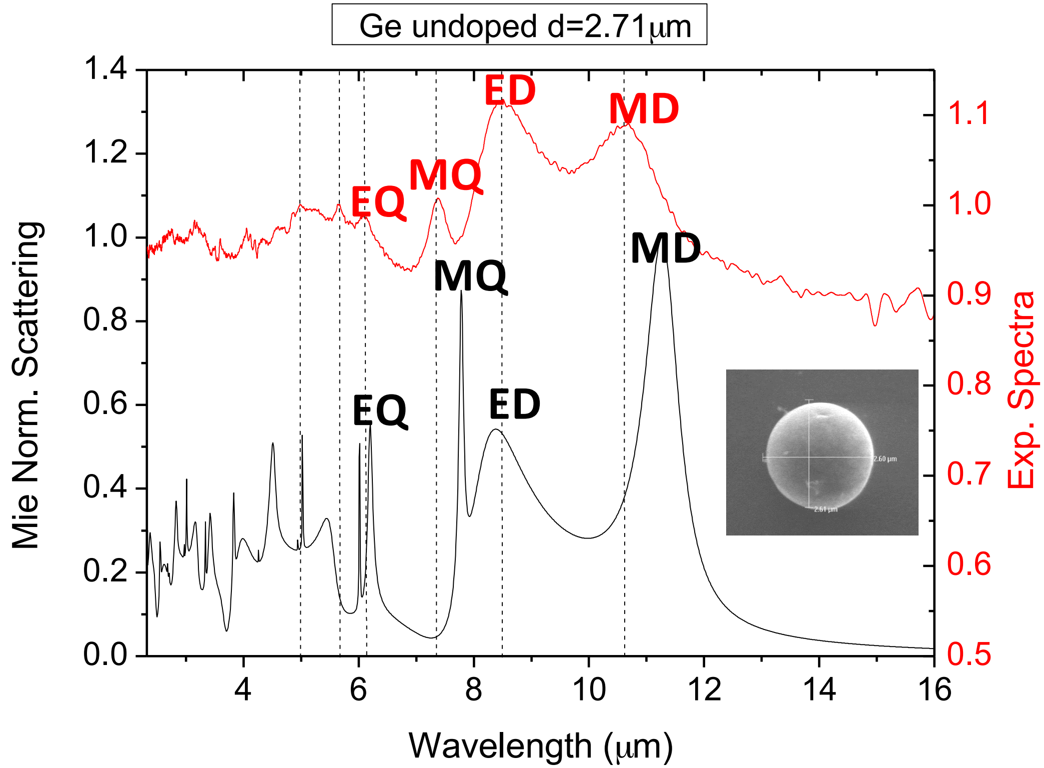

Magnetic dipole (MD)

Electric dipole (ED)

Magnetic quadrupole (MQ)

Electric quadrupole (EQ)

Basic Concept & Principle Challenges

Transmit Array

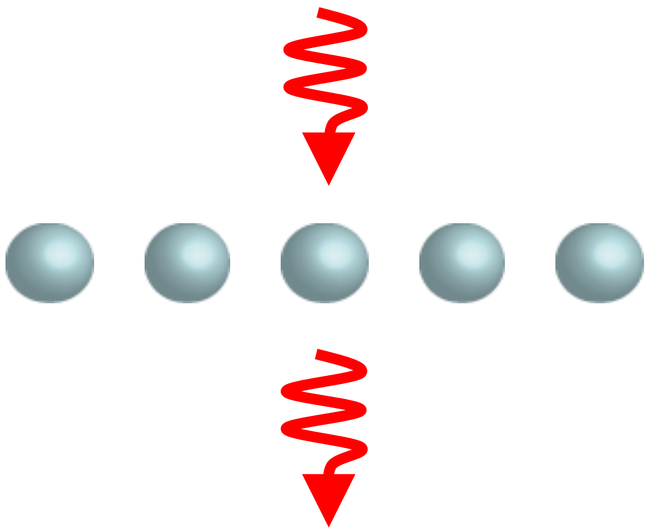

See work by e.g. Grbic, Kivshar, Staude, and Valentine

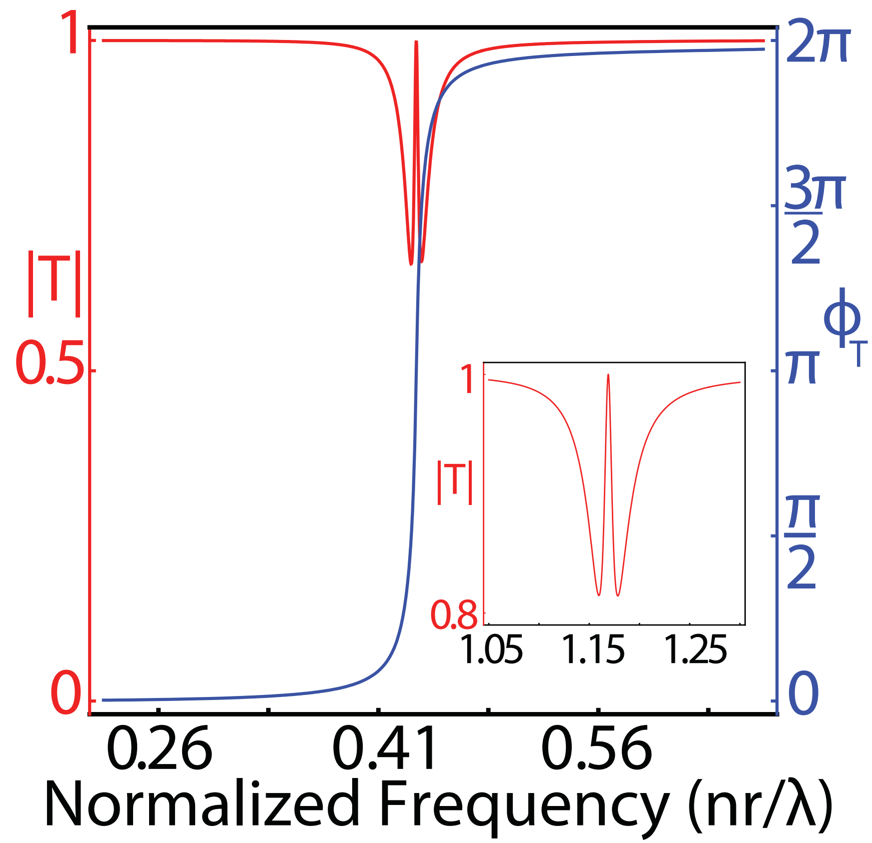

- Goal: Continuous tuning between 0 and 2π with minimal change in amplitude
- Challenge: Metasurface elements are subwavelength with modest Qs (~ 10)
- Requirement: Very large index tuning (Δn~1) needed to shift by 1 linewidth

P.Iyer, N.A. Butakov, and J.A. Schuller *ACS Photonics* **2,** 1077 (2015)

Outline

Prasad Iyer

❶ **Electrically Reconfigurable Metasurfaces (InSb)**

Dr. Tomer Lewi

❷ **Extreme Thermal Tuning of Mie Resonators (PbTe)**

Doping Induced Index Shifts

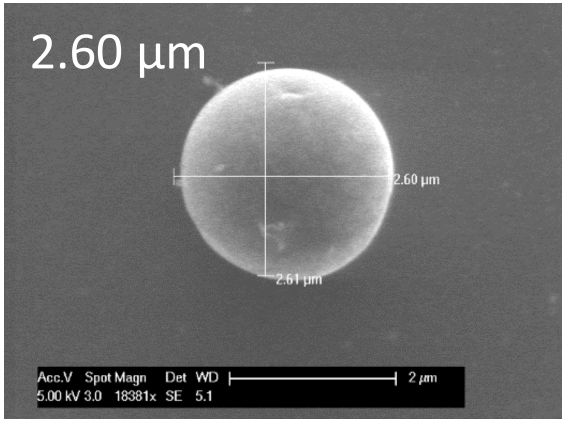

Technique originally developed by Chichkov and Luk'yanchuk groups

Si

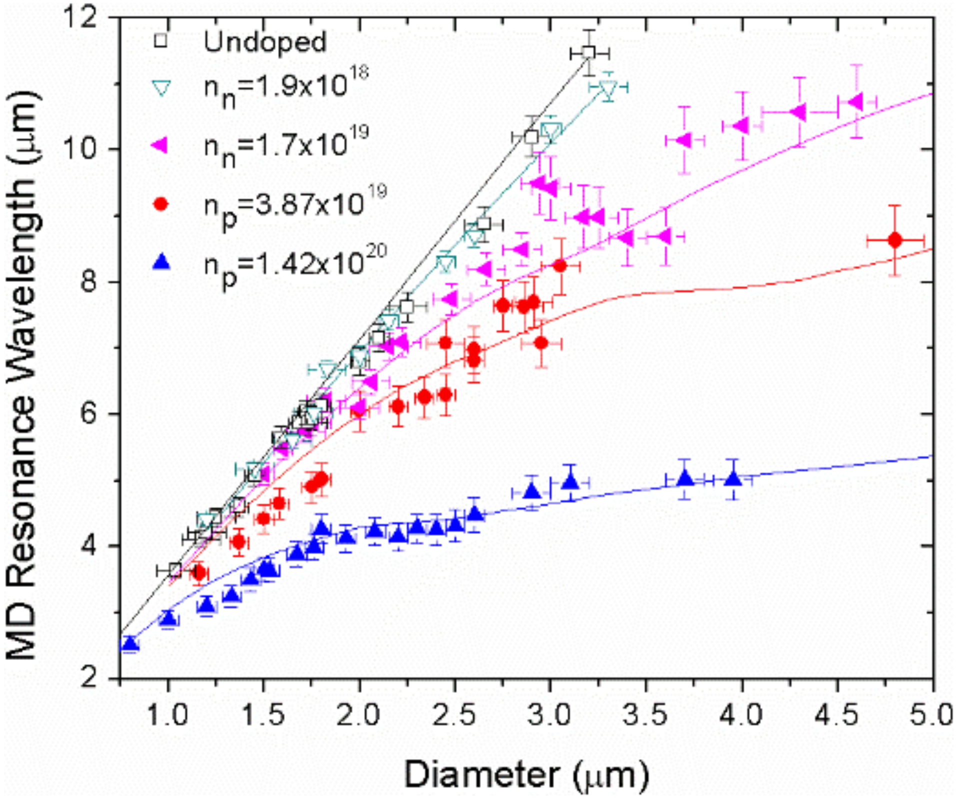

- Resonance wavelength shift increase with increase in wavelength
- Results match Drude models with ***no free parameters***
- **Continuous index tuning from 4 down to 0 (metallic regime)**

T. Lewi, P.P.Iyer, N.A. Butakv, A. Mikhailovsky, and J.A. Schuller *Nano Lett.* **15**, 8188 (2015)

Free-Carrier Refraction: InSb & InAs

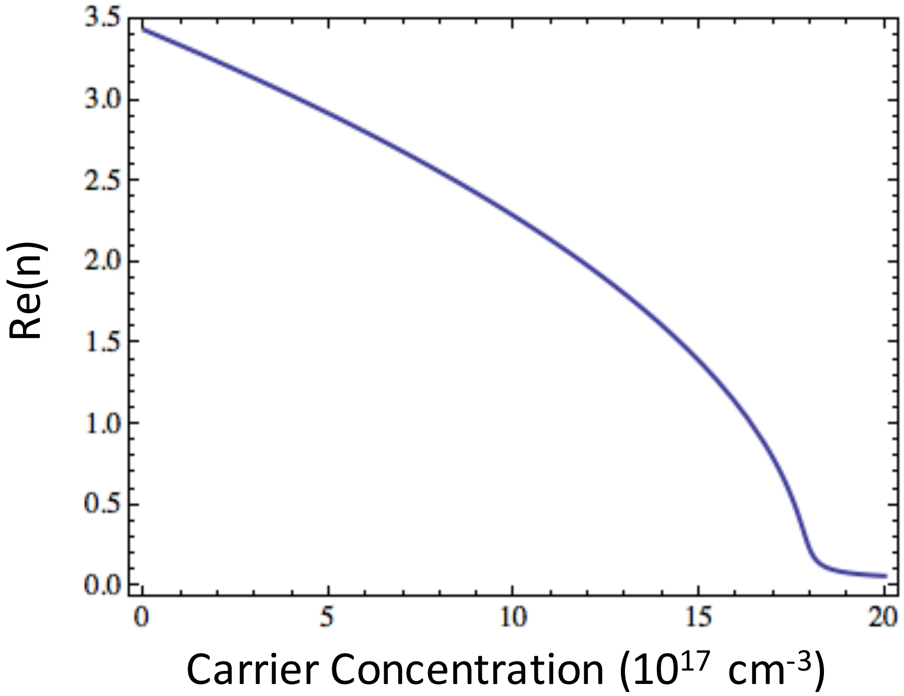

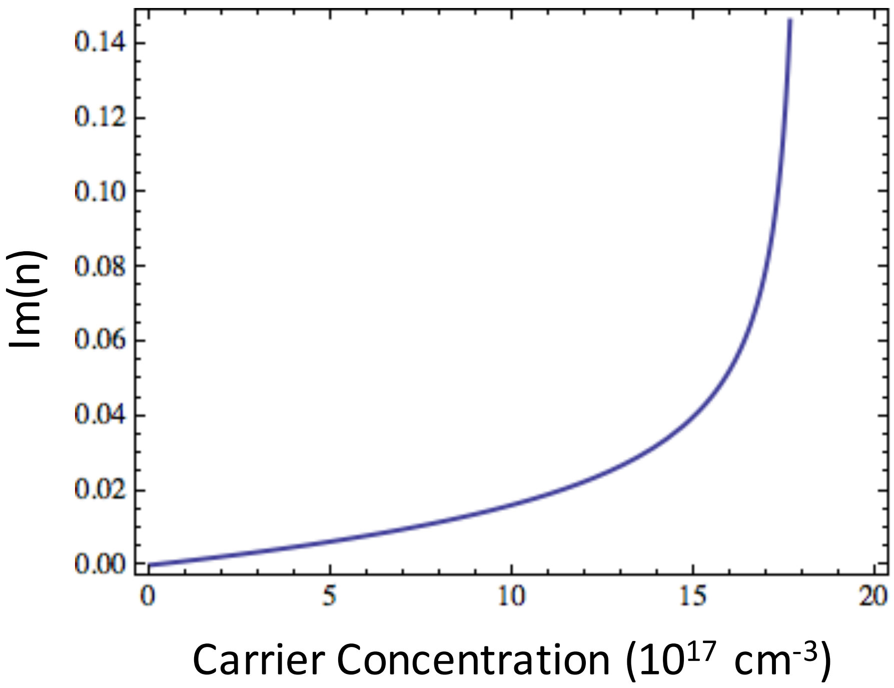

- Note: Doping dependent (e.g. Soref) models overestimate losses
- @ 10.6 µm interesting effects btwn 10^{17} and 10^{18} carriers per cm^3
- Scaling with wavelength: $\mathrm{Re}[n] \propto \lambda^2$ $\mathrm{Im}[n] \propto \lambda^3$

Implementation: InSb Reflectarrays

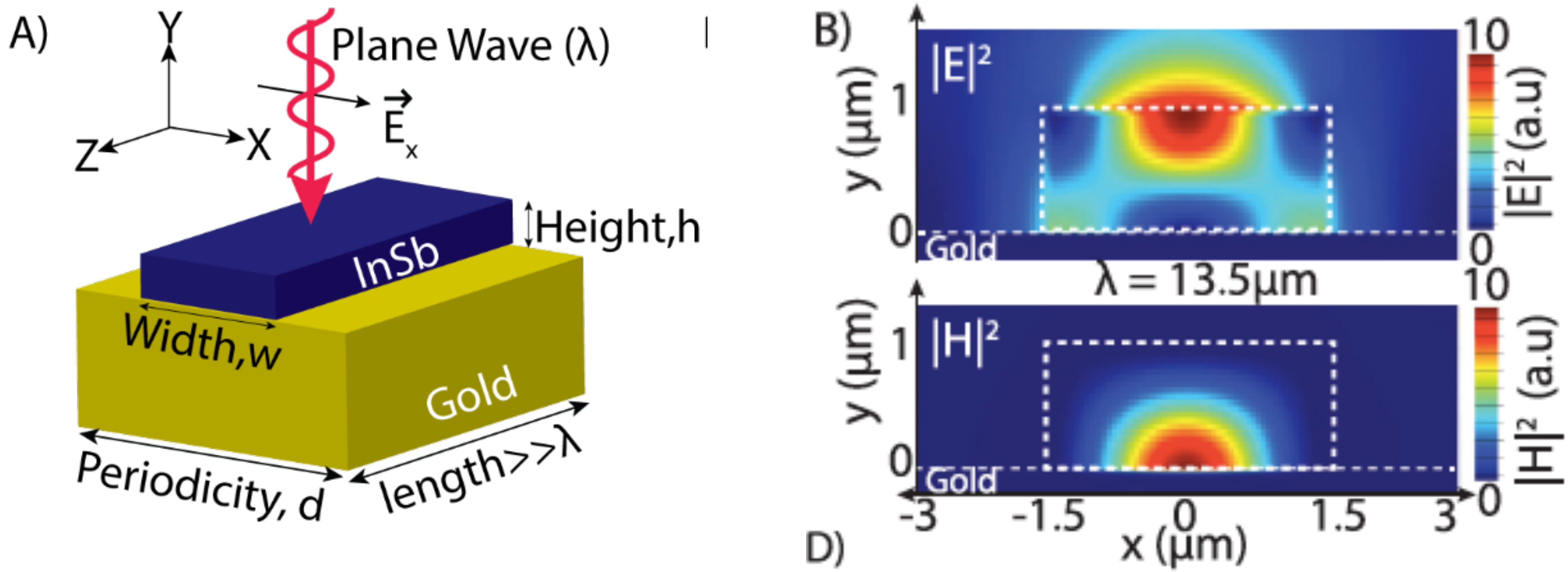

- Our current approach: 1D InSb resonators on reflecting substrate
- Interaction of MD resonance with image dipole ➔ 2π phase shift
- Electric field intensity concentrated near top of resonator

P.P. Iyer, M. Pendharkar, and J.A. Schuller *Adv. Opt. Mater.* **4,** 1582 (2016)

Aside: Limits of Depletion-Mode Devices

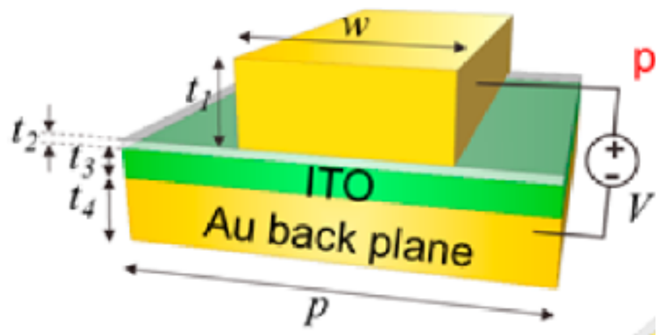

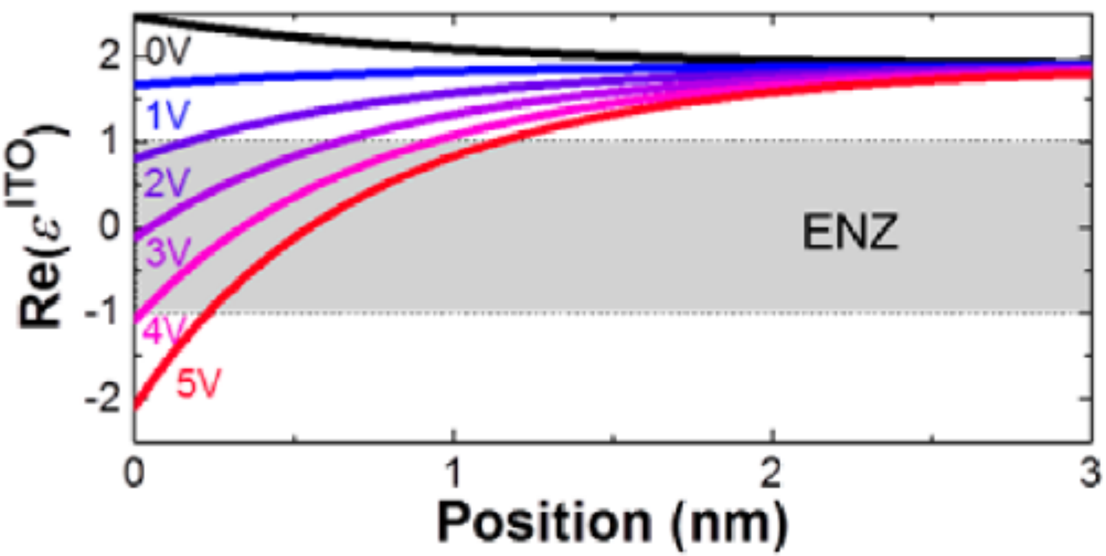

Y.W. Huang, *Nano Lett.* **16,** 5319 (2016)

- Depletion-mode devices (e.g. ITO or graphene) exhibit inherent tradeoff between carrier density and modulation width

$$W = \sqrt{\frac{2\varepsilon V}{qN}}$$

Mie Resonators: Experiments

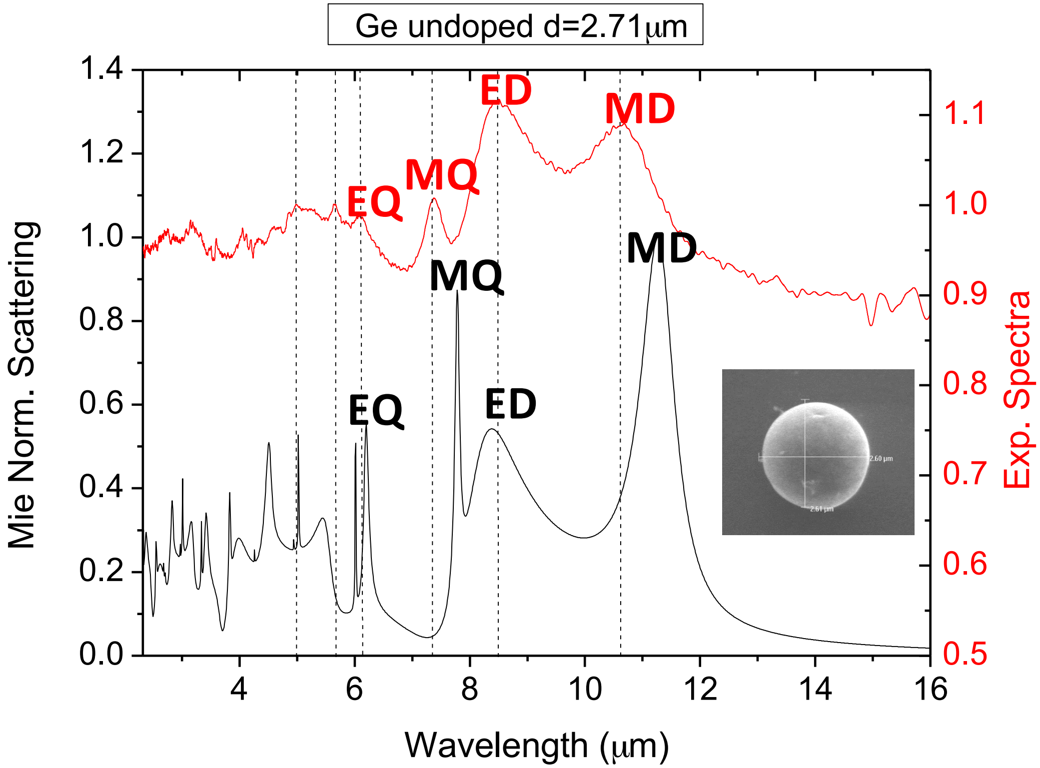

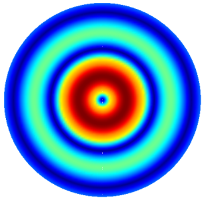

Magnetic dipole (MD)

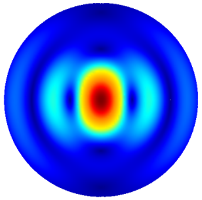

Electric dipole (ED)

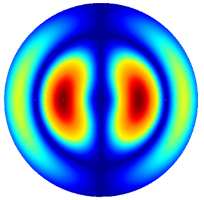

Magnetic quadrupole (MQ)

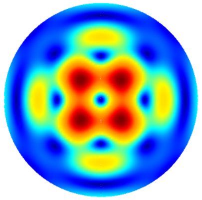

Electric quadrupole (EQ)

Solution: Forward Biased Heterojunction

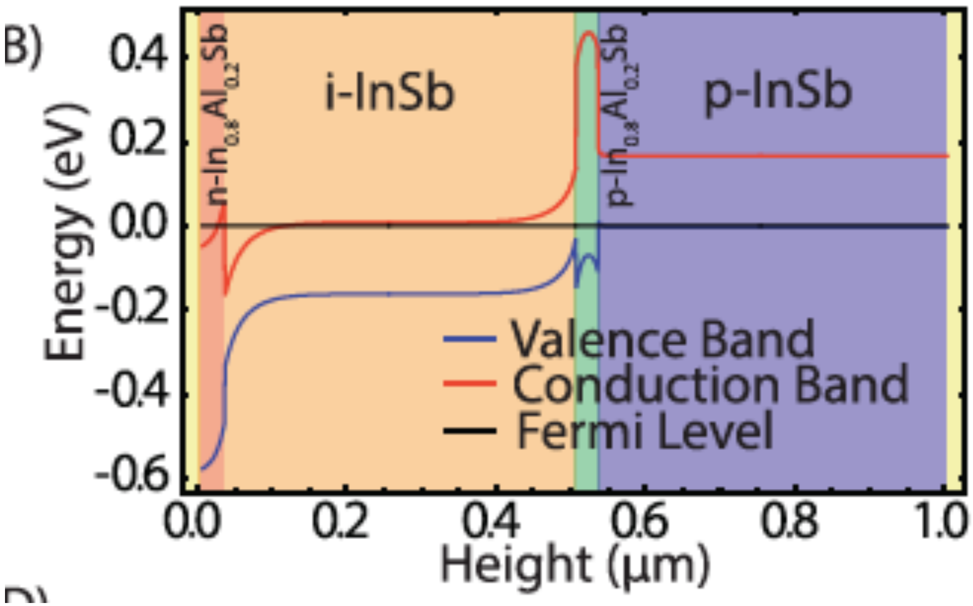

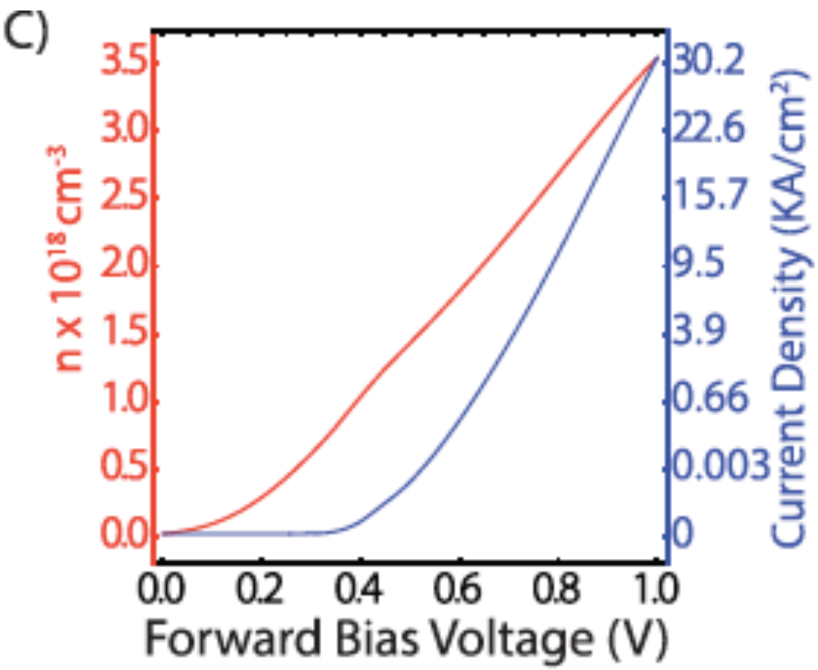

- Homojunction in forward bias does not reach high enough carrier densities
- InAlSb acts as hole and electron blocking layers

P.P. Iyer, M. Pendharkar, and J.A. Schuller *Adv. Opt. Mater.* **4,** 1582 (2016)

Solution: Forward Biased Heterojunction

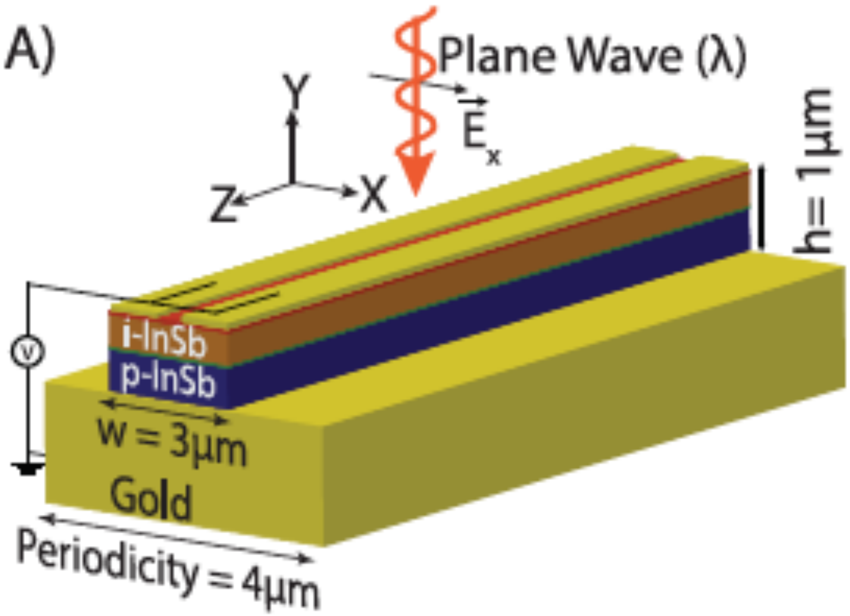

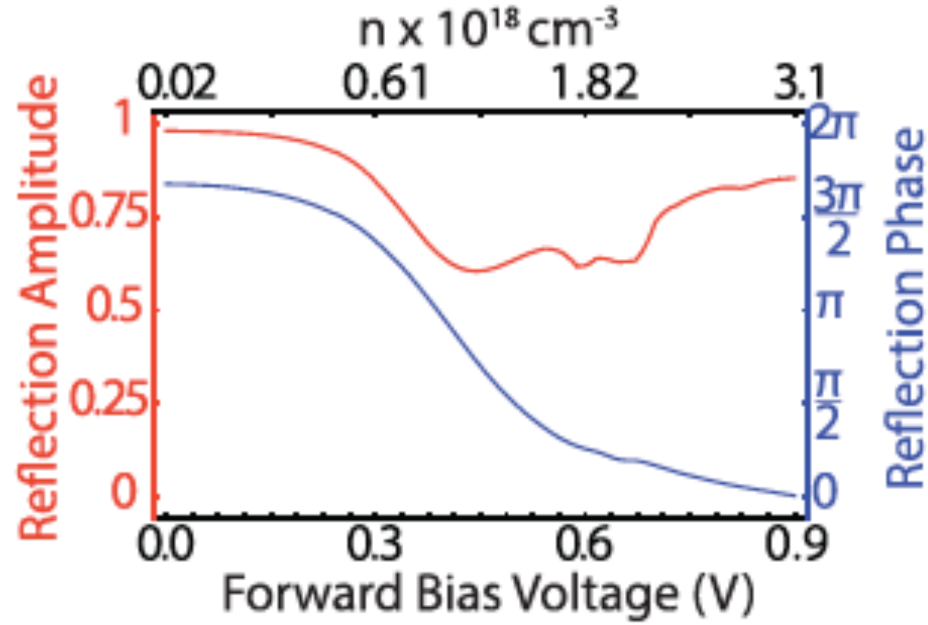

- Homojunction in forward bias does not reach high enough carrier densities
- InAlSb acts as hole and electron blocking layers
- Nearly 2π phase shift w/ minimal change in reflection amplitude

P.P. Iyer, M. Pendharkar, and J.A. Schuller *Adv. Opt. Mater.* **4,** 1582 (2016)

Phased Array Simulations

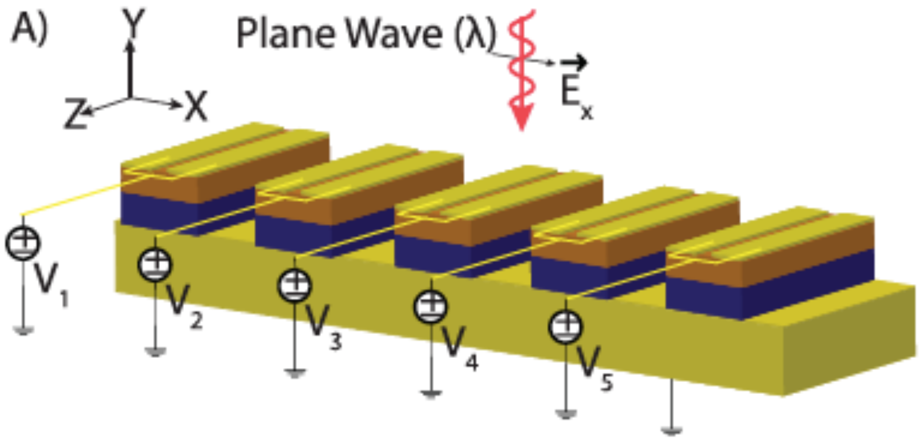

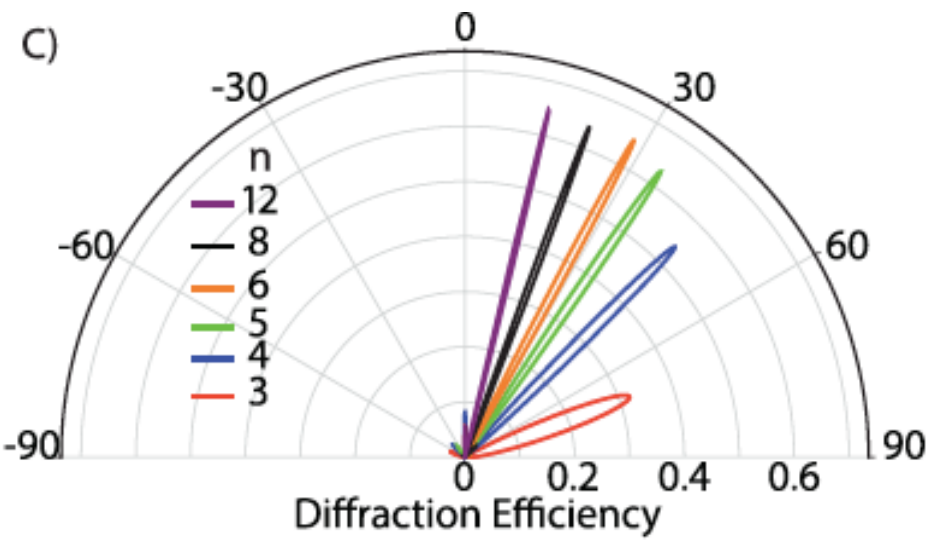

- Array enables continuous beam steering over nearly 180°
- 60% of incident energy diffracted into desired lobe
- **n=12:** Case of maximum possible phase error

P.P. Iyer, M. Pendharkar, and J.A. Schuller *Adv. Opt. Mater.* **4,** 1582 (2016)

Experimental Results: Device Stack

Repeat	Thickness	Layer	Doping
	15nm	n++ InAs	Si : $2x10^{18}cm^{-3}$
5X	1nm	n-$InAl_{0.55}As_{0.45}$	Si : $2x10^{18}cm^{-3}$
	1nm	i-InAs	
5X	1nm	n-$InAl_{0.5}As_{0.5}$	Si : $2x10^{18}cm^{-3}$
	1nm	i-InAs	
5X	1nm	n-$InAl_{0.45}As_{0.55}$	Si : $2x10^{18}cm^{-3}$
	1nm	i-InAs	
5X	1nm	n-$InAl_{0.4}As_{0.6}$	Si : $2x10^{18}cm^{-3}$
	1nm	i-InAs	
5X	1nm	n-$InAl_{0.35}As_{0.65}$	Si : $2x10^{18}cm^{-3}$
	1nm	i-InAs	
	1.25µm	i-InAs	
41X	1nm	p-$Al_{0.5}Ga_{0.5}Sb$	Be : $2x10^{18}cm^{-3}$
	1nm	i-AlSb	
	10nm	p++GaSb	Si : $4x10^{18}cm^{-3}$
	1.25µm	n++ InAs	Si : $5x10^{19}cm^{-3}$
	500nm	i-GaSb Buffer	
	500µm	GaSb Substrate	Te : $1x10^{17}cm^{-3}$

P.P. Iyer, M. Pendharkar, C.J. Palmstrom, and J.A. Schuller (unpublished)

Experimental Results: Device Stack

Repeat	Thickness	Layer	Doping
	15nm	n++ InAs	Si : 2x10^{18}cm^{-3}
5X	1nm	n-InAl$_{0.55}$As$_{0.45}$	Si : 2x10^{18}cm^{-3}
	1nm	i-InAs	
5X	1nm	n-InAl$_{0.5}$As$_{0.5}$	Si : 2x10^{18}cm^{-3}
	1nm	i-InAs	
5X	1nm	n-InAl$_{0.45}$As$_{0.55}$	Si : 2x10^{18}cm^{-3}
	1nm	i-InAs	
5X	1nm	n-InAl$_{0.4}$As$_{0.6}$	Si : 2x10^{18}cm^{-3}
	1nm	i-InAs	
5X	1nm	n-InAl$_{0.35}$As$_{0.65}$	Si : 2x10^{18}cm^{-3}
	1nm	i-InAs	
	1.25µm	i-InAs	
41X	1nm	p-Al$_{0.5}$Ga$_{0.5}$Sb	Be : 2x10^{18}cm^{-3}
	1nm	i-AlSb	
	10nm	p++GaSb	Si : 4x10^{18}cm^{-3}
	1.25µm	n++ InAs	Si : 5x10^{19}cm^{-3}
	500nm	i-GaSb Buffer	
	500µm	GaSb Substrate	Te : 1x10^{17}cm^{-3}

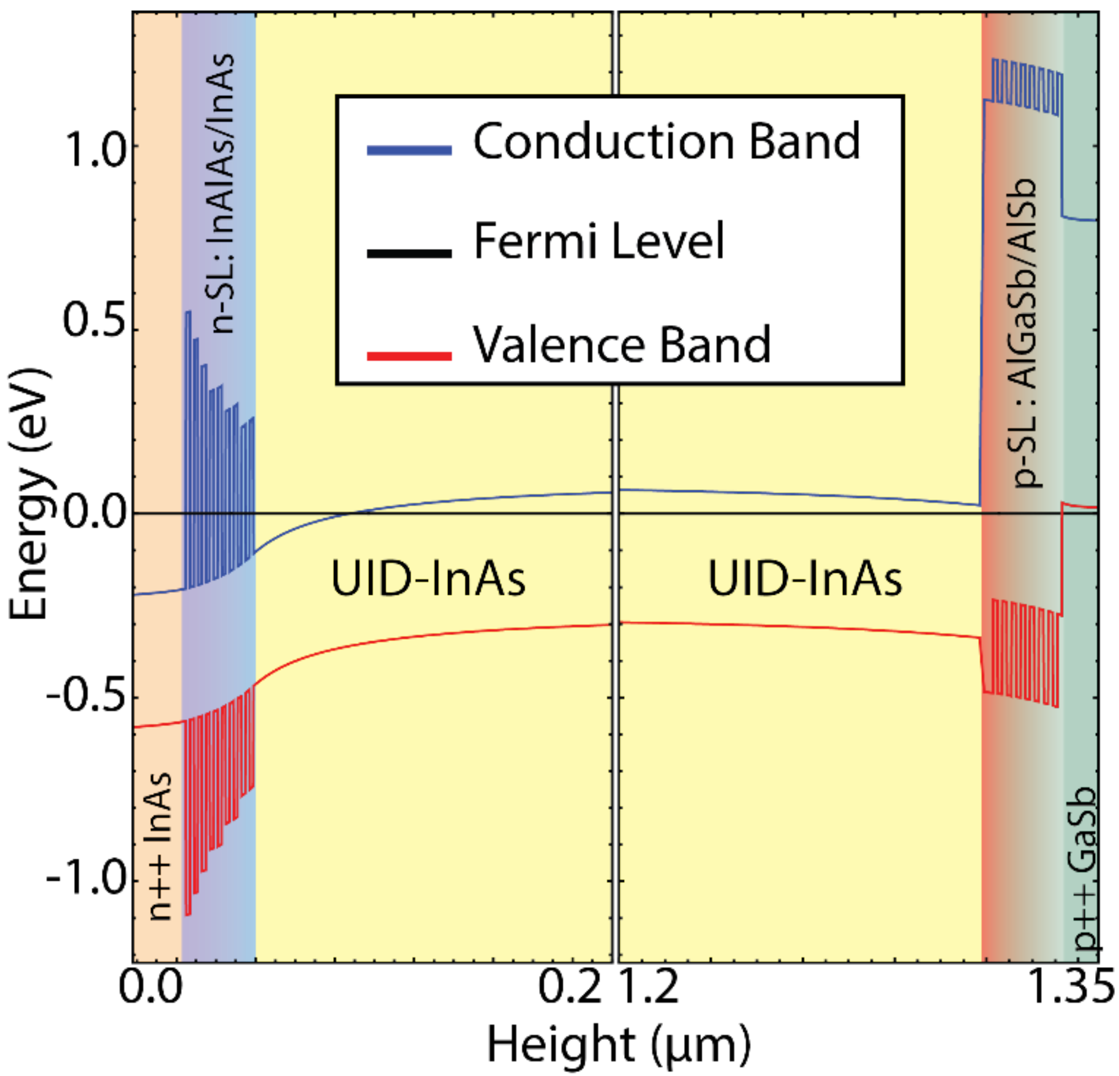

P.P. Iyer, M. Pendharkar, C.J. Palmstrom, and J.A. Schuller (unpublished)

Experimental Results: Fabrication

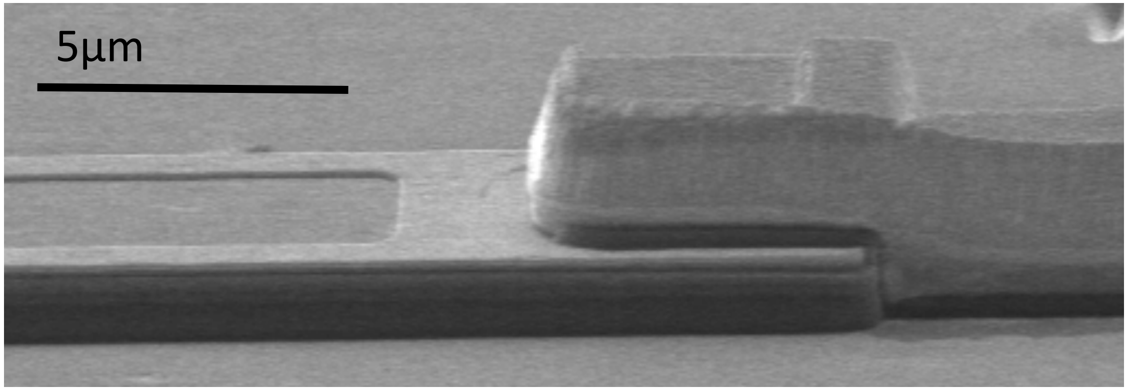

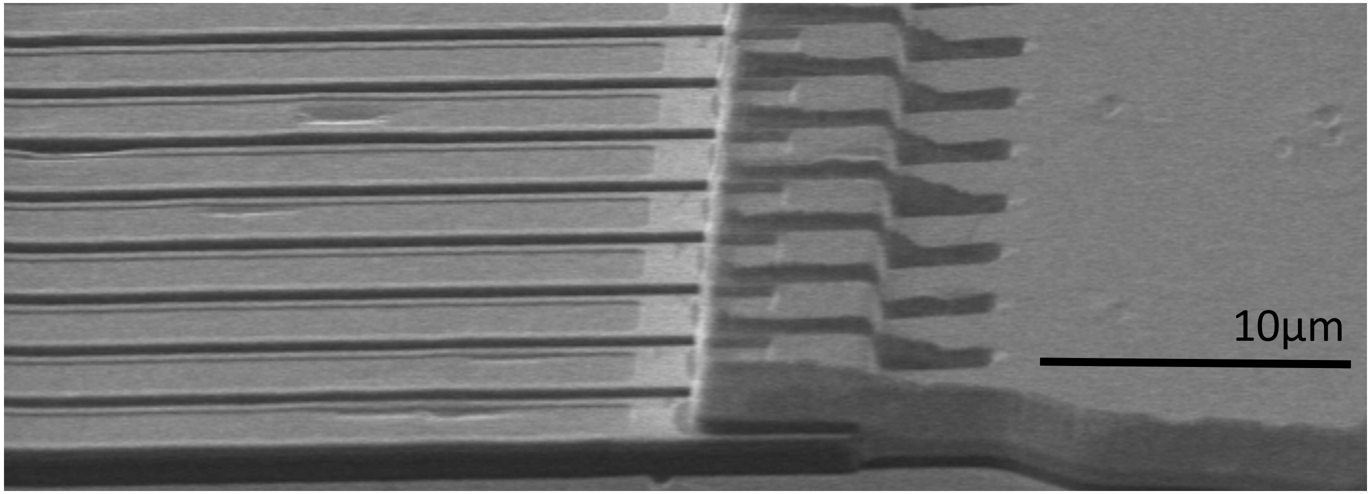

- Metallic clusters currently prevent array measurements

P.P. Iyer, M. Pendharkar, C.J. Palmstrom, and J.A. Schuller (unpublished)

Experimental Results: Tunable MetaAtoms!

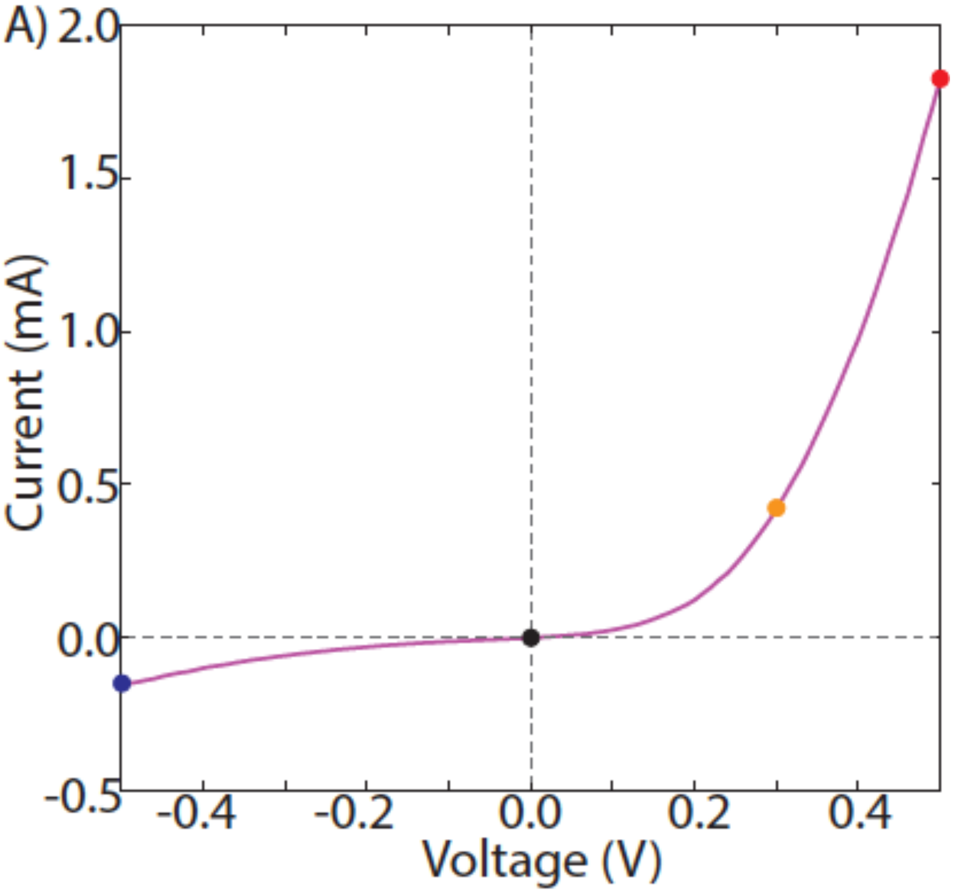

P.P. Iyer, M. Pendharkar, C.J. Palmstrom, and J.A. Schuller (unpublished)

Experimental Results: Tunable MetaAtoms!

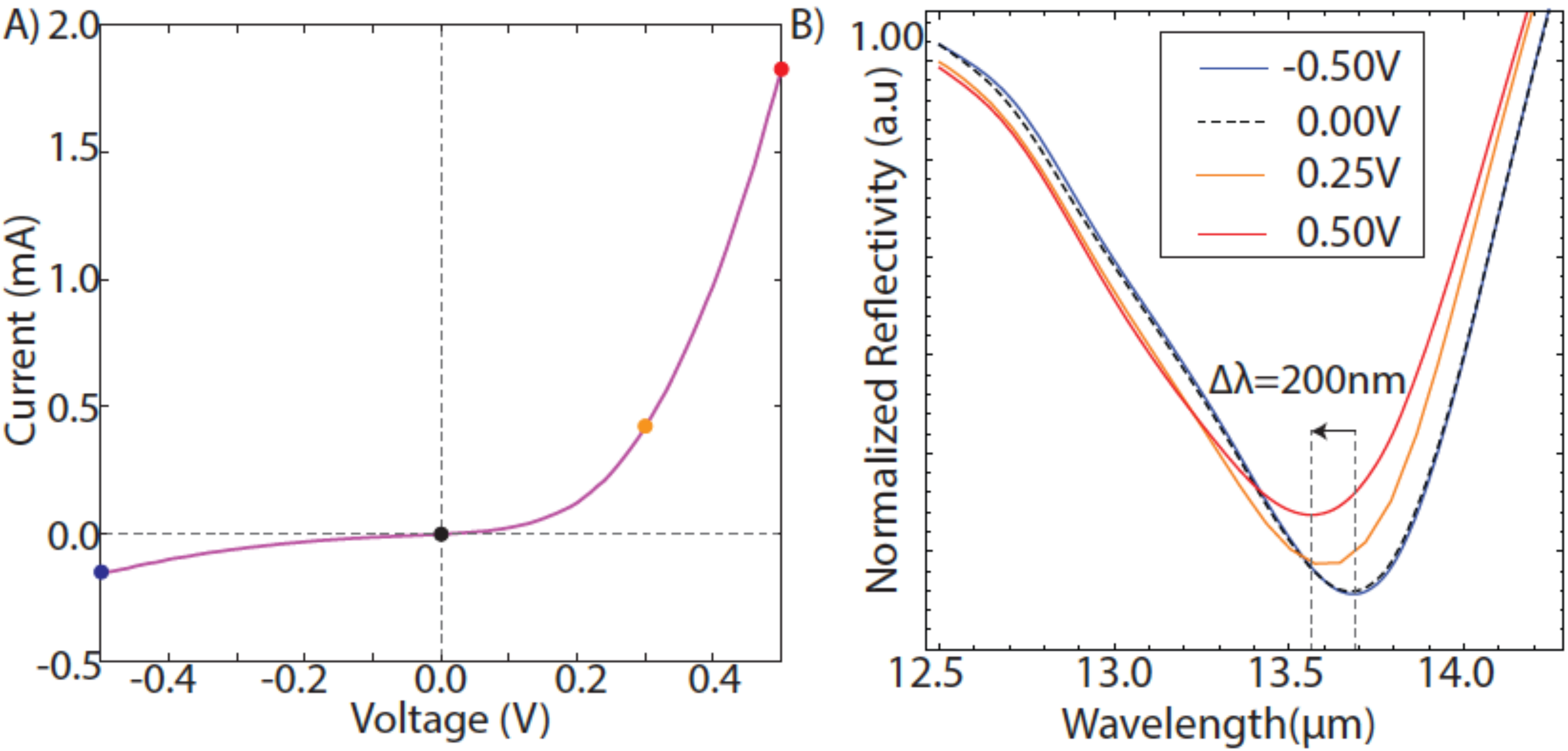

- Δλ=200nm ➔ΔΦ ~ π in arrays

P.P. Iyer, M. Pendharkar, C.J. Palmstrom, and J.A. Schuller (unpublished)

Outline

Prasad Iyer

❶ Electrically Reconfigurable Metasurfaces (InSb)

- We demonstrate electrically reconfigurable metasurfaces and metaresonators with low loss and high diffraction efficiency

❷ Extreme Thermal Tuning of Mie Resonators (PbTe)

Dr. Tomer Lewi

Experimental Results: InSb Plasmons

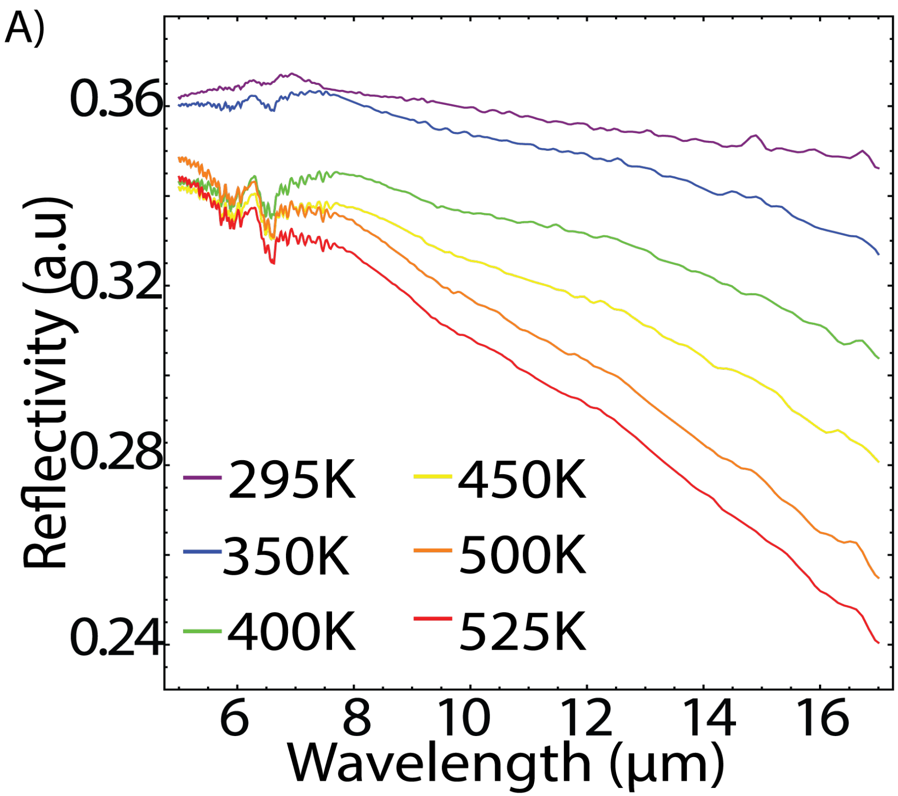

$$\varepsilon(\omega) = \varepsilon_{\infty} - \frac{ne^2}{\varepsilon_0 m_{eff} \omega^2}$$

- Infer optical constants from fits of IR Reflectivity to Drude models
- Free-carrier refraction turns on rapidly around 300 K

P.P. Iyer, M. Pendharkar, C.J. Palmstrom, and J.A. Schuller *Nature Comm.* **8,** 472 (2017).

Experimental Results: InSb Plasmons

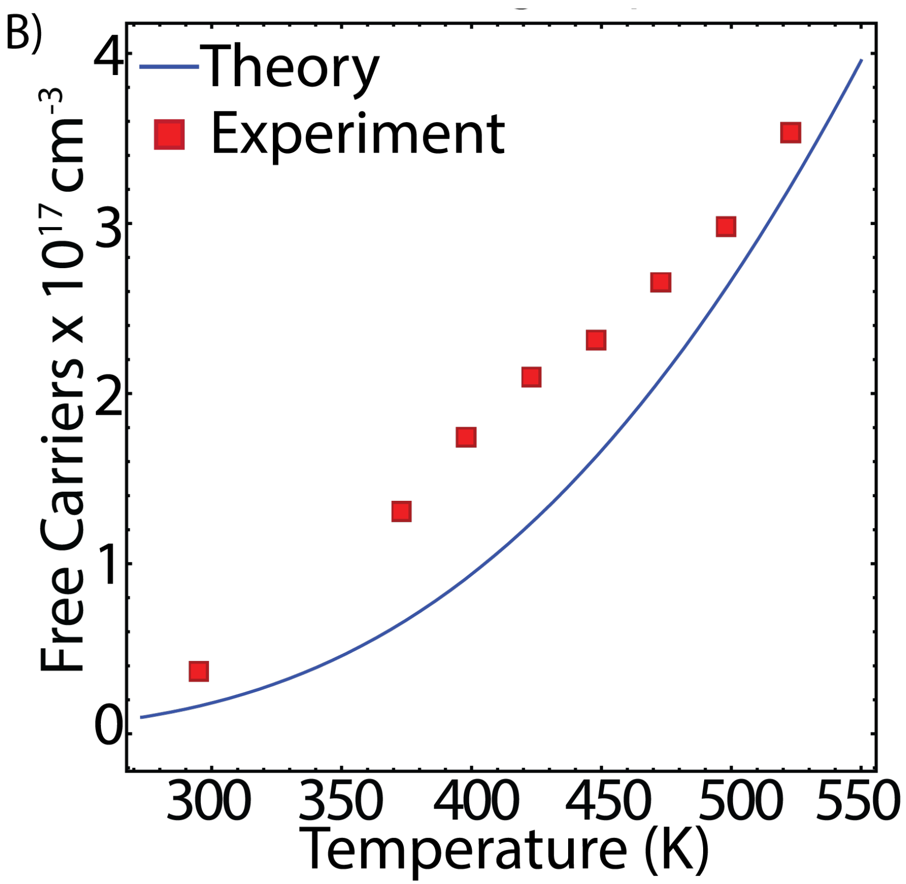

$$\varepsilon(\omega) = \varepsilon_\infty - \frac{ne^2}{\varepsilon_0 m_{eff} \omega^2}$$

- Infer optical constants from fits of IR Reflectivity to Drude models
- Free-carrier refraction turns on rapidly around 300 K

P.P. Iyer, M. Pendharkar, C.J. Palmstrom, and J.A. Schuller *Nature Comm.* **8,** 472 (2017).

Experimental Results: InSb Plasmons

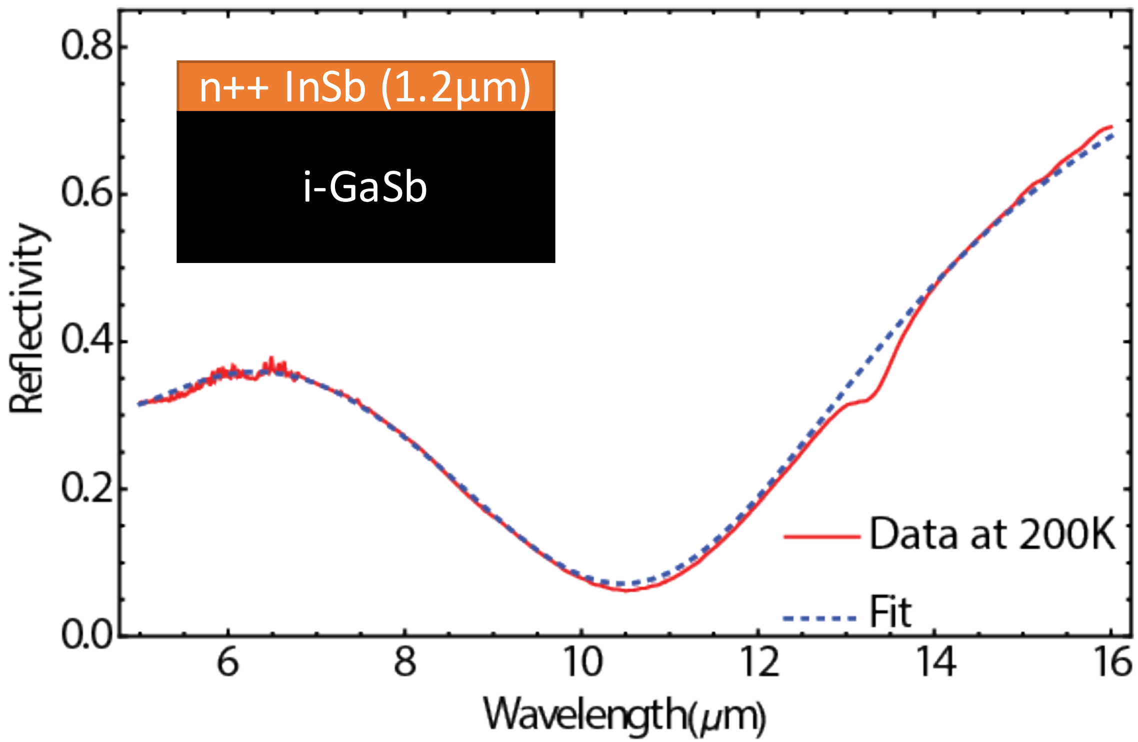

$$\varepsilon(\omega) = \varepsilon_\infty - \frac{ne^2}{\varepsilon_0 m_{eff} \omega^2}$$

- Infer optical constants from fits of IR Reflectivity to Drude models
- $6*10^{18}$ cm^{-3} produces plasma frequency at approx. 13 µm

P.P. Iyer, M. Pendharkar, C.J. Palmstrom, and J.A. Schuller *Nature Comm.* **8,** 472 (2017).

InSb Plasmons Temperature Dependence

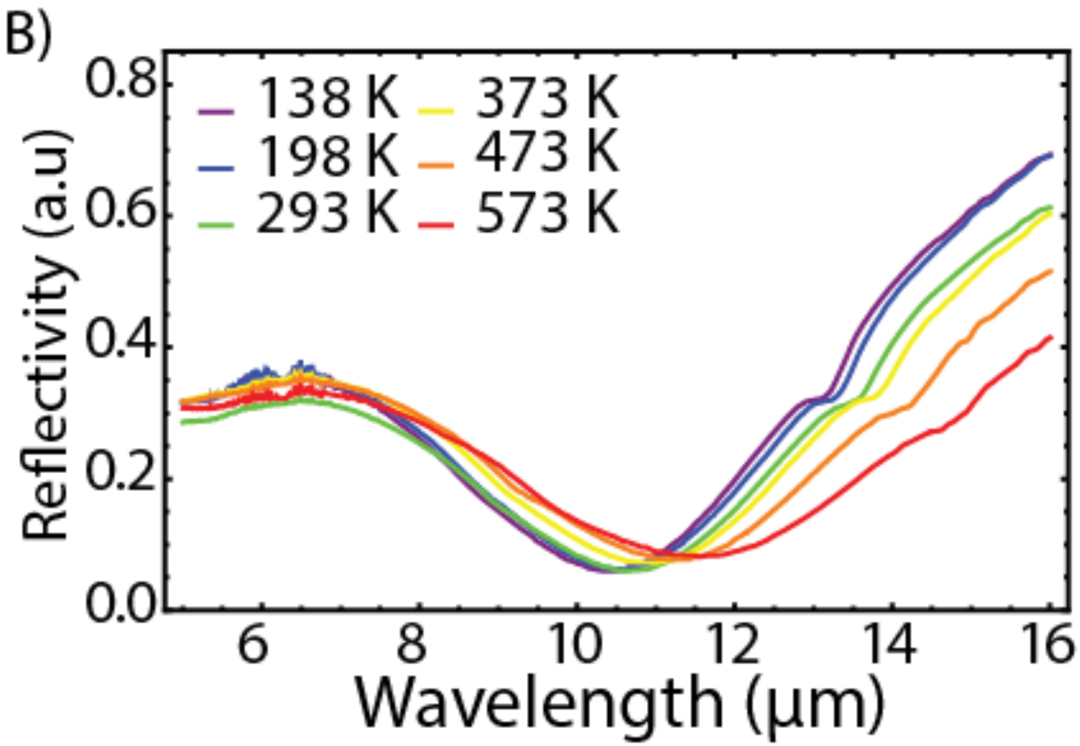

$$\varepsilon(\omega) = \varepsilon_\infty - \frac{ne^2}{\varepsilon_0 m_{eff} \omega^2}$$

- Infer optical constants from fits of IR Reflectivity to Drude models
- Heating sample **red-shifts** plasma frequency

P.P. Iyer, M. Pendharkar, C.J. Palmstrom, and J.A. Schuller *Nature Comm.* **8,** 472 (2017).

InSb Plasmons Temperature Dependence

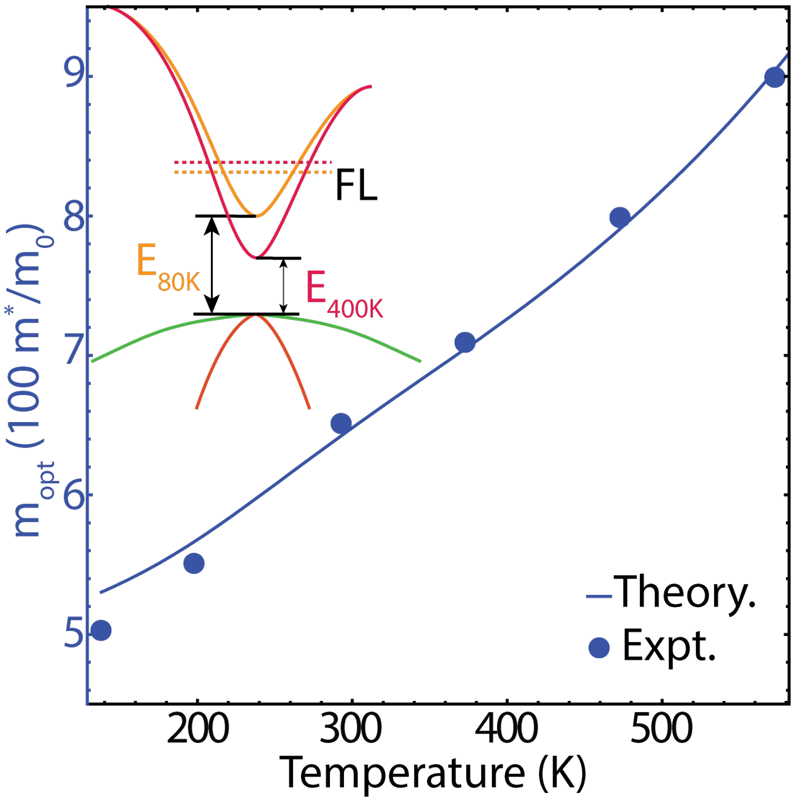

$$\varepsilon(\omega) = \varepsilon_\infty - \frac{ne^2}{\varepsilon_0 m_{eff} \omega^2}$$

$$m_{n=0}[T] = m_{n=0}[T=0]\sqrt{1+4\alpha kT}$$

$$m_n[T] = m_{n=0}\sqrt{1+\frac{1}{2}\left(\frac{3}{\pi}\right)^{2/3}\frac{h^2 n^{2/3}}{eE_g m_{n=0}}}$$

- Infer optical constants from fits of IR Reflectivity to Drude models
- Heating sample **red-shifts** plasma frequency
- Average electron effective mass changes by factor of 2
- Can this be actuated by non-thermal means? (see e.g. work of R.P.H. Chang)

Outline

Prasad Iyer

❶ Electrically Reconfigurable Metasurfaces (InSb)

- We demonstrate electrically reconfigurable metasurfaces and metaresonators with low loss and high diffraction efficiency
- Effective mass tuning provides a new approach for dynamically modulating plasmonic properties

Acknowledgments

- **MBE growth by Mihir Pendharkar and Chris Palmstrom (UCSB)**

Outline

Prasad Iyer

❶ Electrically Reconfigurable Metasurfaces (InSb)

- We theoretically demonstrate electrically reconfigurable metasurfaces with low loss and high diffraction efficiency
- We experimentally demonstrate free-carrier tuning based on both **concentration** and **mass**

Dr. Tomer Lewi

❷ Extreme Thermal Tuning of Mie Resonators (PbTe)

Thermal Tuning of Mie Resonators (Ge)

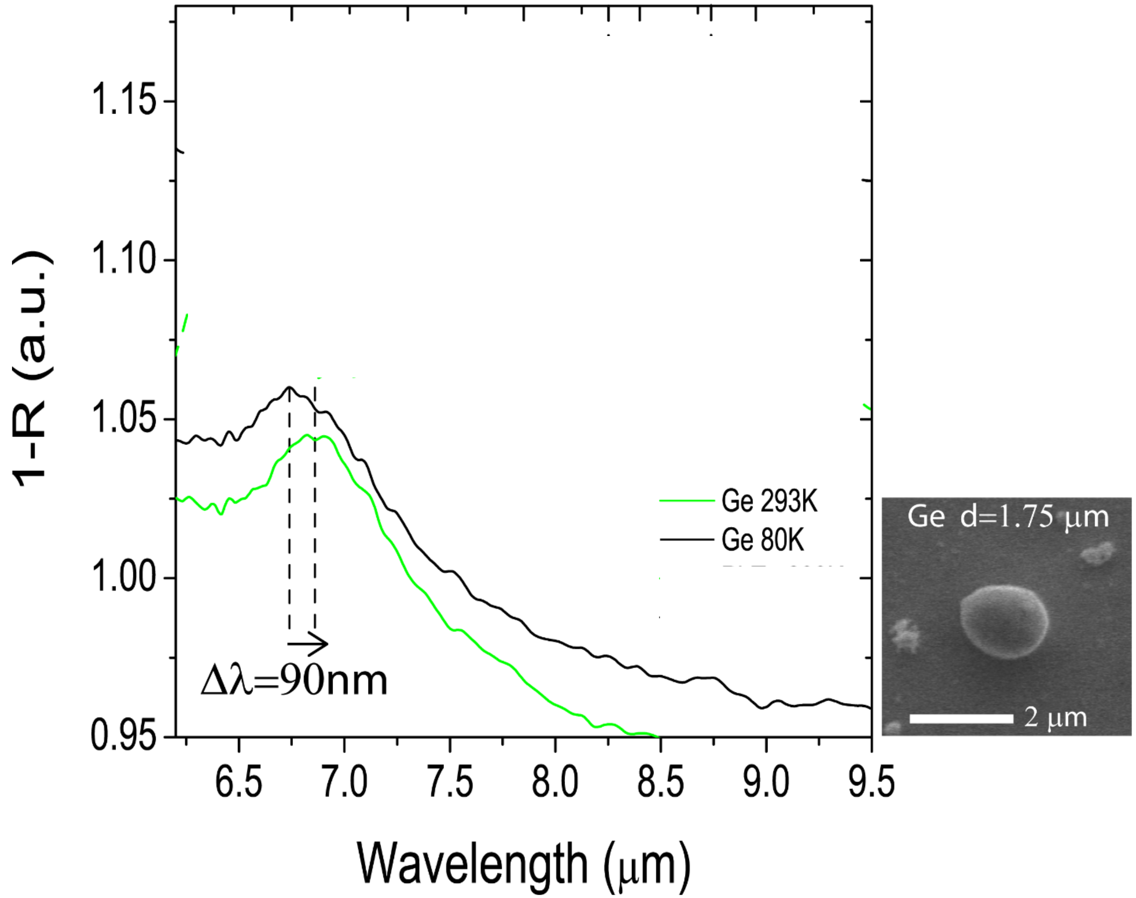

- Ge has largest thermo-optic coefficient of any group IV or III-V semiconductor

Thermal Tuning of Mie Resonators (PbTe)

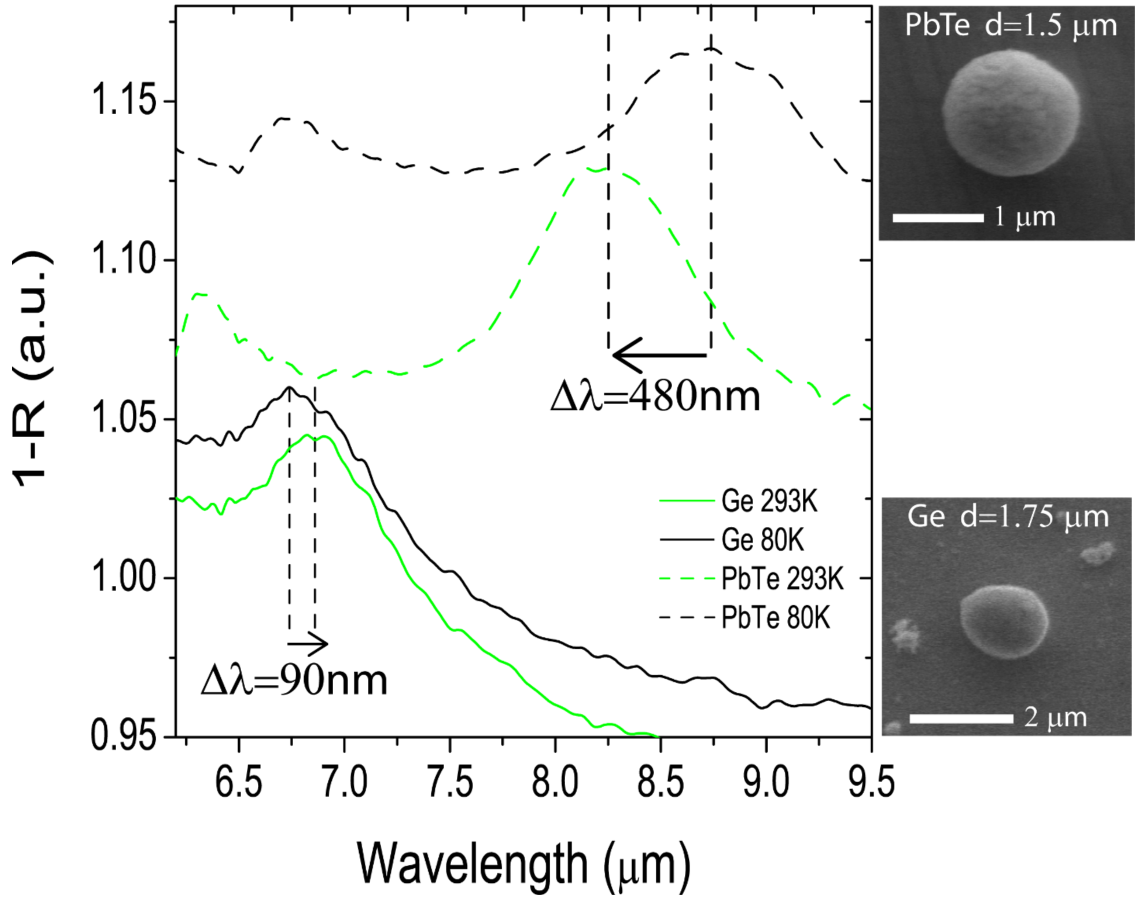

- Ge has largest thermo-optic coefficient of any group IV or III-V semiconductor
- PbTe: **huge index** (n~6) w/ **anomalous sign and magnitude** of thermo-optic effect

T. Lewi, et al. *Nano Lett.*. **17**, 3940 (2017)

Thermal Tuning of Mie Resonators (PbTe)

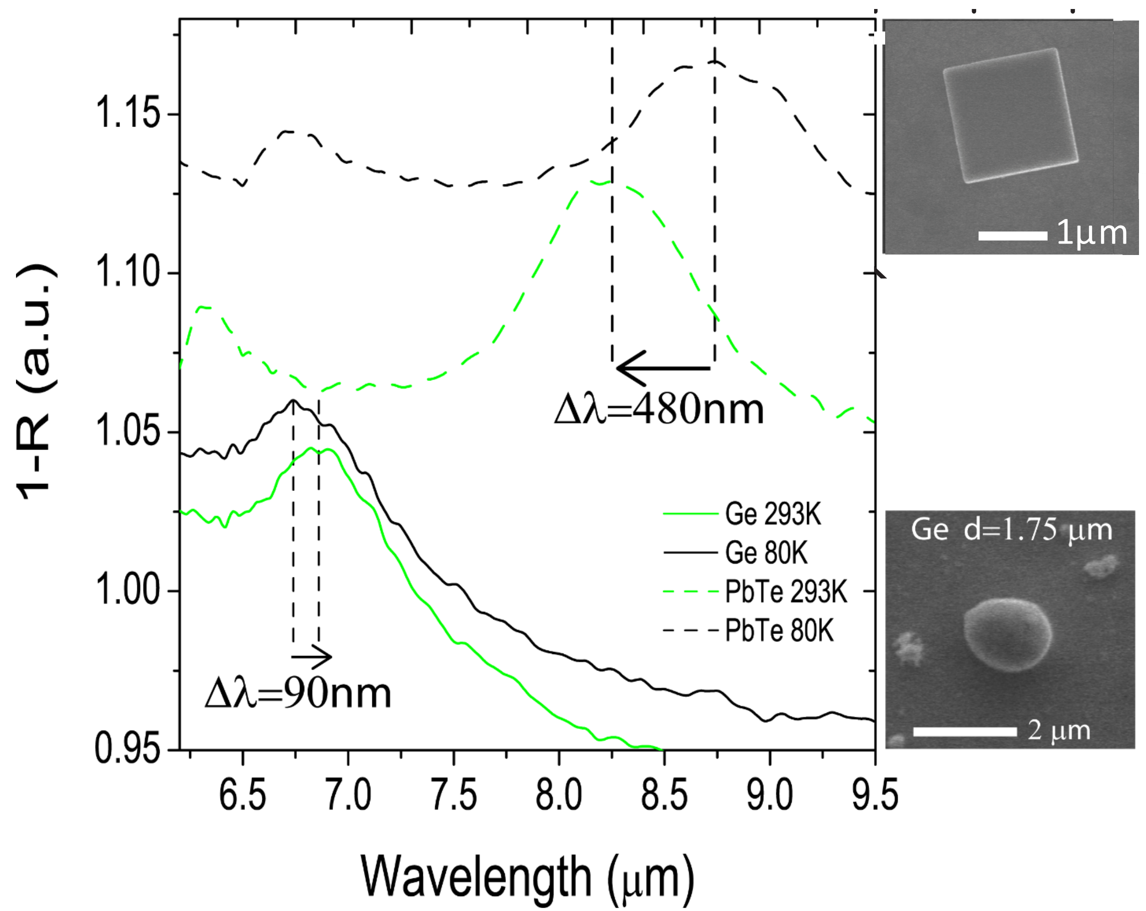

- Ge has largest thermo-optic coefficient of any group IV or III-V semiconductor
- PbTe: **huge index** (n~6) w/ **anomalous sign and magnitude** of thermo-optic effect

T. Lewi, et al. *Nano Lett.*. **17**, 3940 (2017)

Tuning by Multiple Linewidths

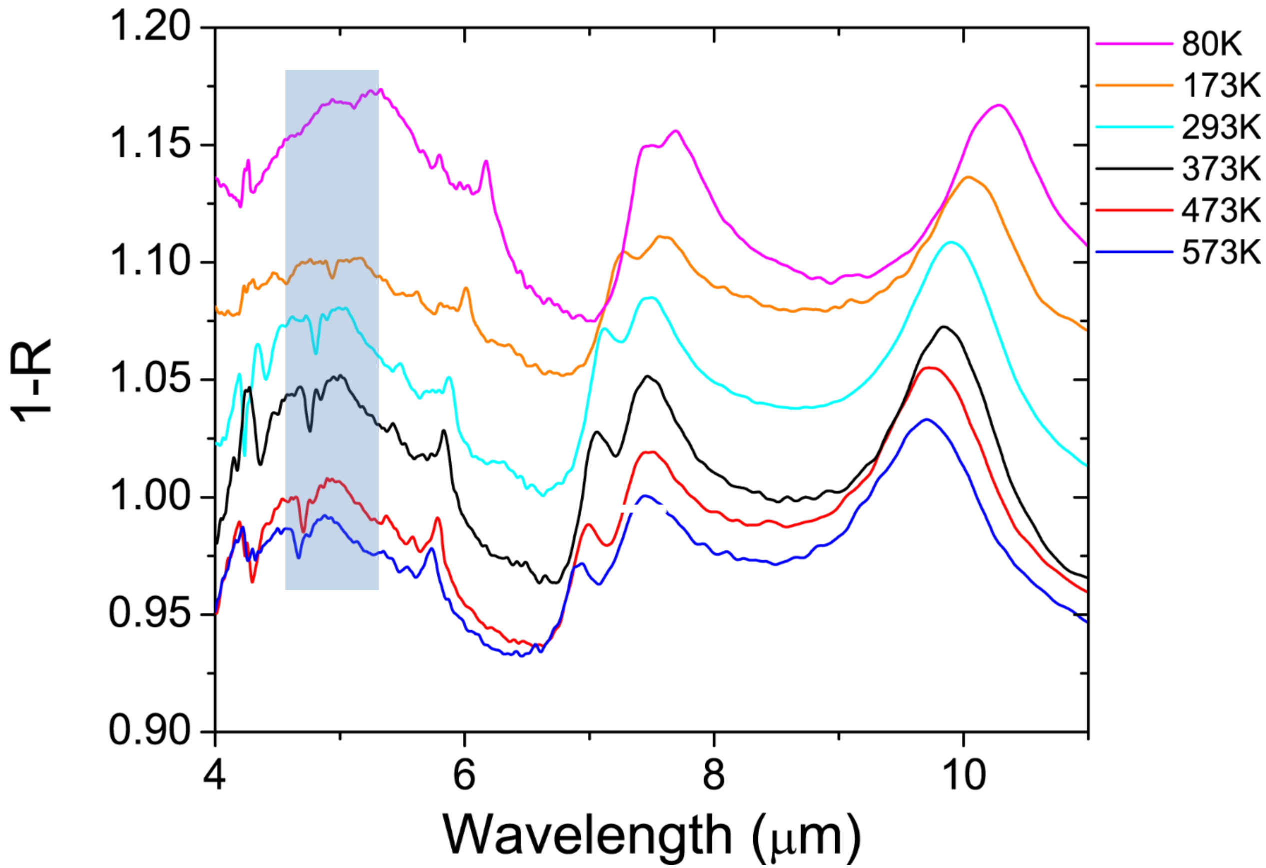

- Higher order, but still subwavelength, modes have far narrower linewidths…
- Enabling tuning by multiple linewidths for same ΔT...

T. Lewi, et al. *Nano Lett.*. **17**, 3940 (2017)

Anomalous Magnitude @ Low Temps

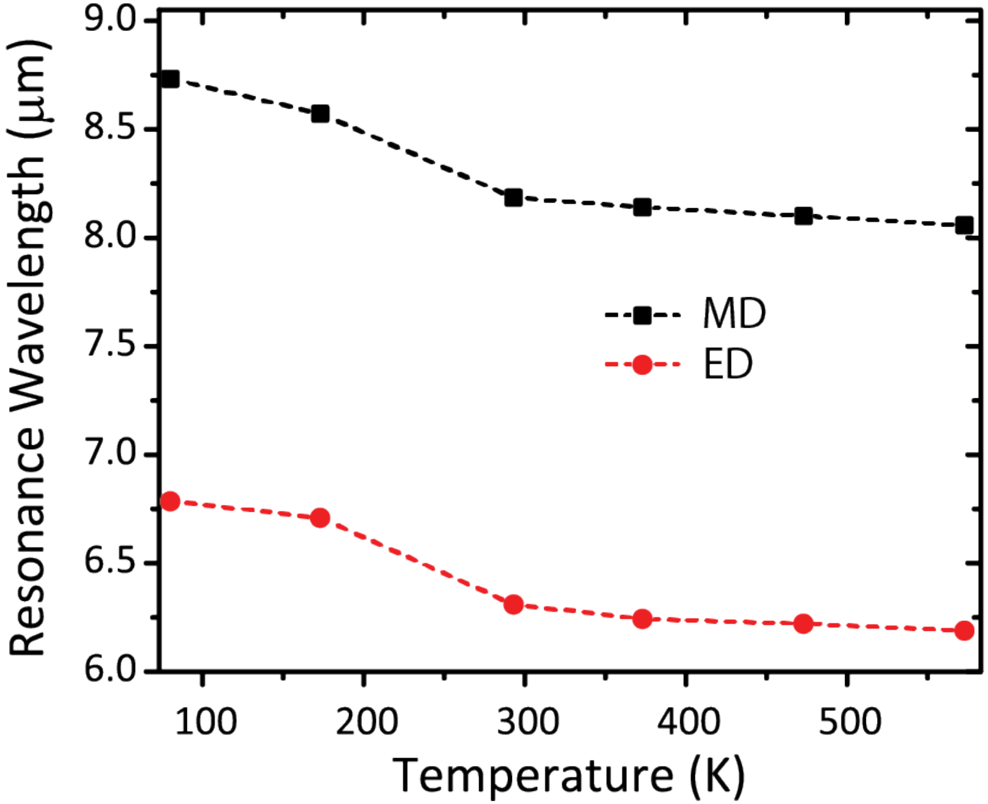

- Higher order, but still subwavelength, modes have far narrower linewidths…
- Enabling tuning by multiple linewidths for same ΔT...
- Coupled with ~ 8 fold increase in TO coefficient at low temps...

T. Lewi, et al. *Nano Lett.*. **17**, 3940 (2017)

Linewidth Tuning w ΔT=10K

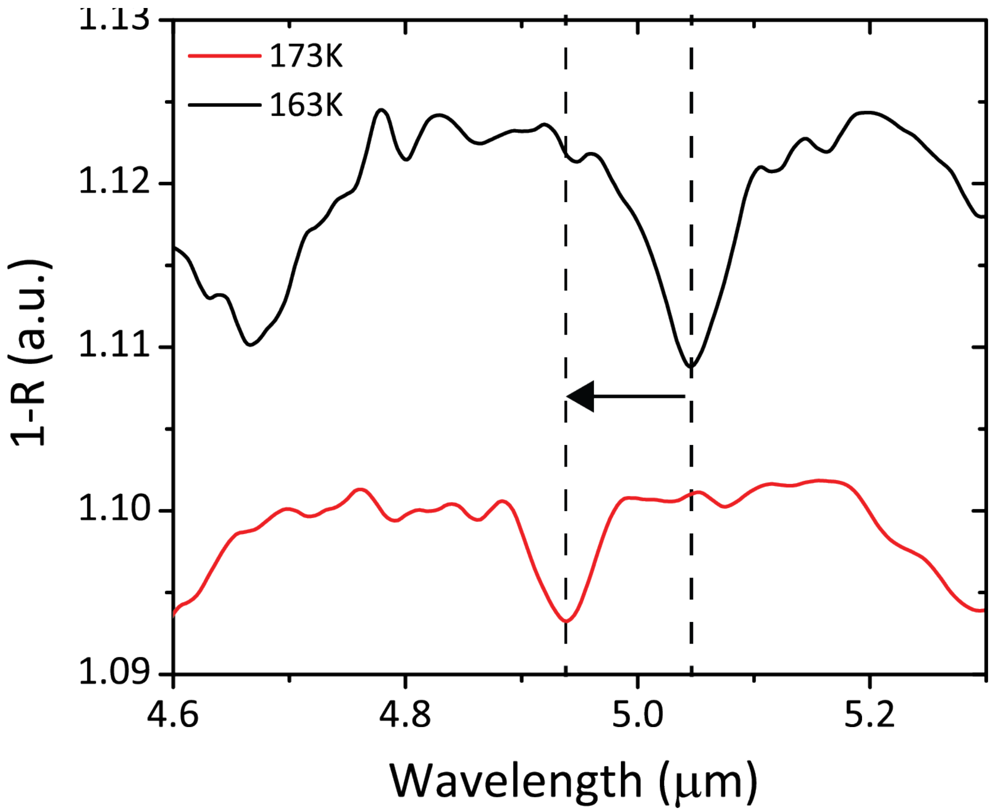

- Higher order, but still subwavelength, modes have far narrower linewidths…
- Enabling tuning by multiple linewidths for same ΔT...
- Coupled with ~ 8 fold increase in TO coefficient at low temps...
- Enables linewidth tuning with as little as 10K temperature swings!

Tuning by Multiple Linewidths: MetaFilters

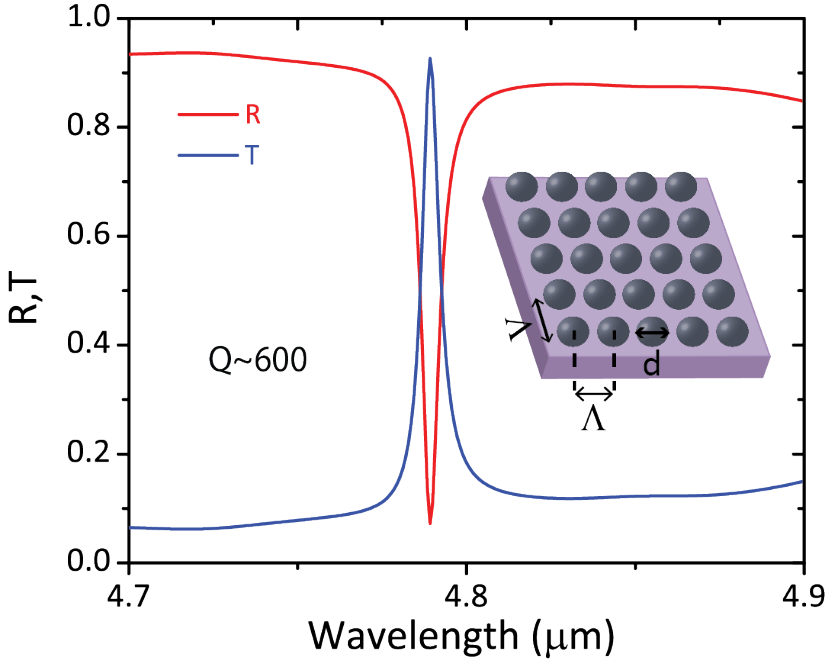

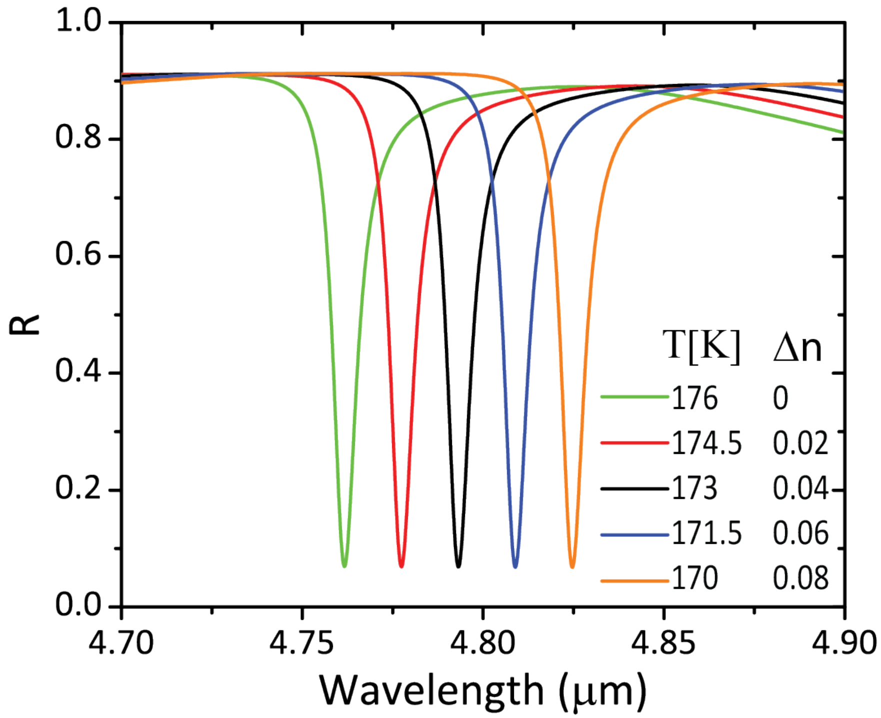

- Higher order, but still subwavelength, modes have far narrower linewidths…
- Enabling tuning by multiple linewidths for same ΔT...
- Coupled with ~ 8 fold increase in TO coefficient at low temps...
- Enables linewidth tuning with as little as 10K temperature swings!

Tuning by Multiple Linewidths: Metasurface

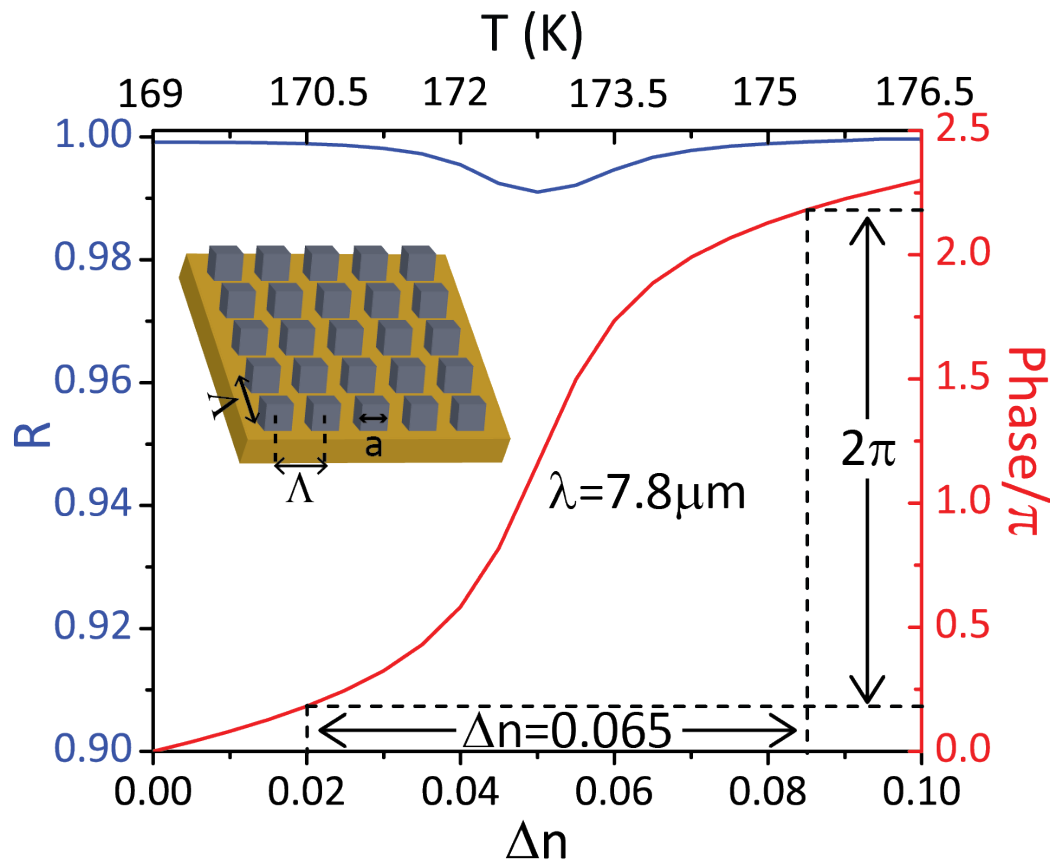

- Higher order, but still subwavelength, modes have far narrower linewidths…
- Enabling tuning by multiple linewidths for same ΔT...
- Coupled with ~ 8 fold increase in TO coefficient at low temps...
- Enables linewidth tuning with as little as 10K temperature swings!

Outline

Prasad Iyer

❶ Electrically Reconfigurable Metasurfaces (InSb)

- We demonstrate electrically reconfigurable metasurfaces and metaresonators with low loss and high diffraction efficiency
- Effective mass tuning provides a new approach for dynamically modulating plasmonic properties

Dr. Tomer Lewi

❷ Extreme Thermal Tuning of Mie Resonators (PbTe)

- PbTe is a solution processable, high refractive index semiconductor with anomalous thermo-optic tunability
- We demonstrate tuning of subwavelength resonances by more than one linewidth with less than 10 K temperature modulation

Outline

❶ Electrically Tunable Semiconductor MetaResonators

- We theoretically demonstrate electrically reconfigurable metasurfaces with low loss and high diffraction efficiency
- We experimentally demonstrate electrically tunable InAs MetaResonators

❷ Thermal Free-carrier Tuning of MetaResonators

- We experimentally demonstrate a novel thermal free-carrier tuning mechanism based on modulating both electron **density** and **mass**
- Thermal free-carrier tuning yields **record-breaking** thermo-optic effects

Acknowledgments

Prasad Iyer
Project Lead

Chris Palmstrom & Mihir Pendharkar
InAs & InSb MBE growth

Bonus Slides

Lattice matched epitaxial growth stack

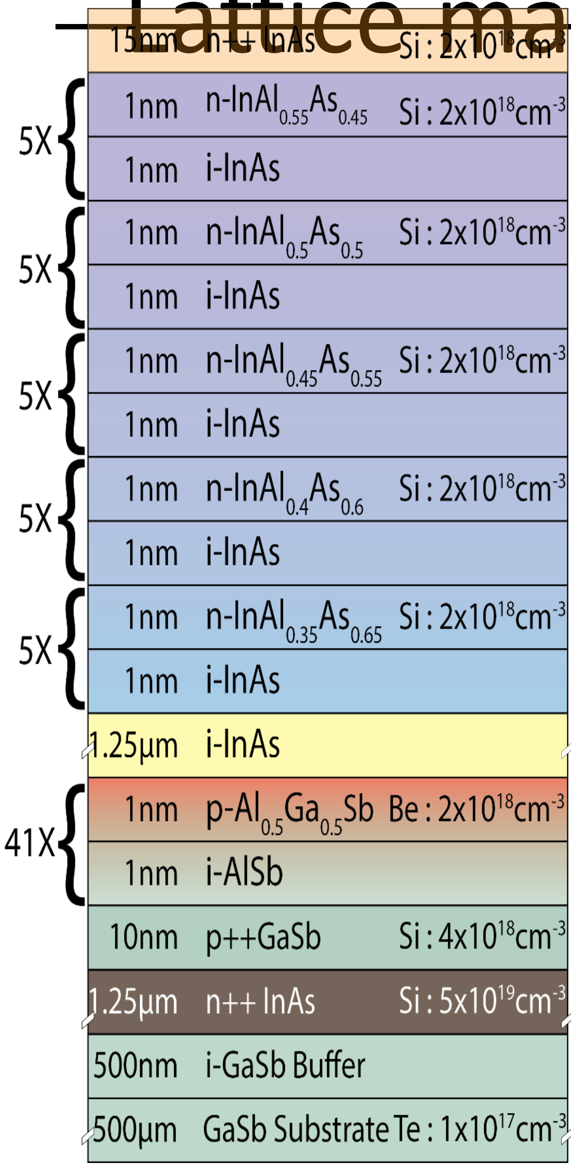

Hole Blocking Super Lattice

Electron Blocking Super Lattice

Reflecting Metallic Substrate

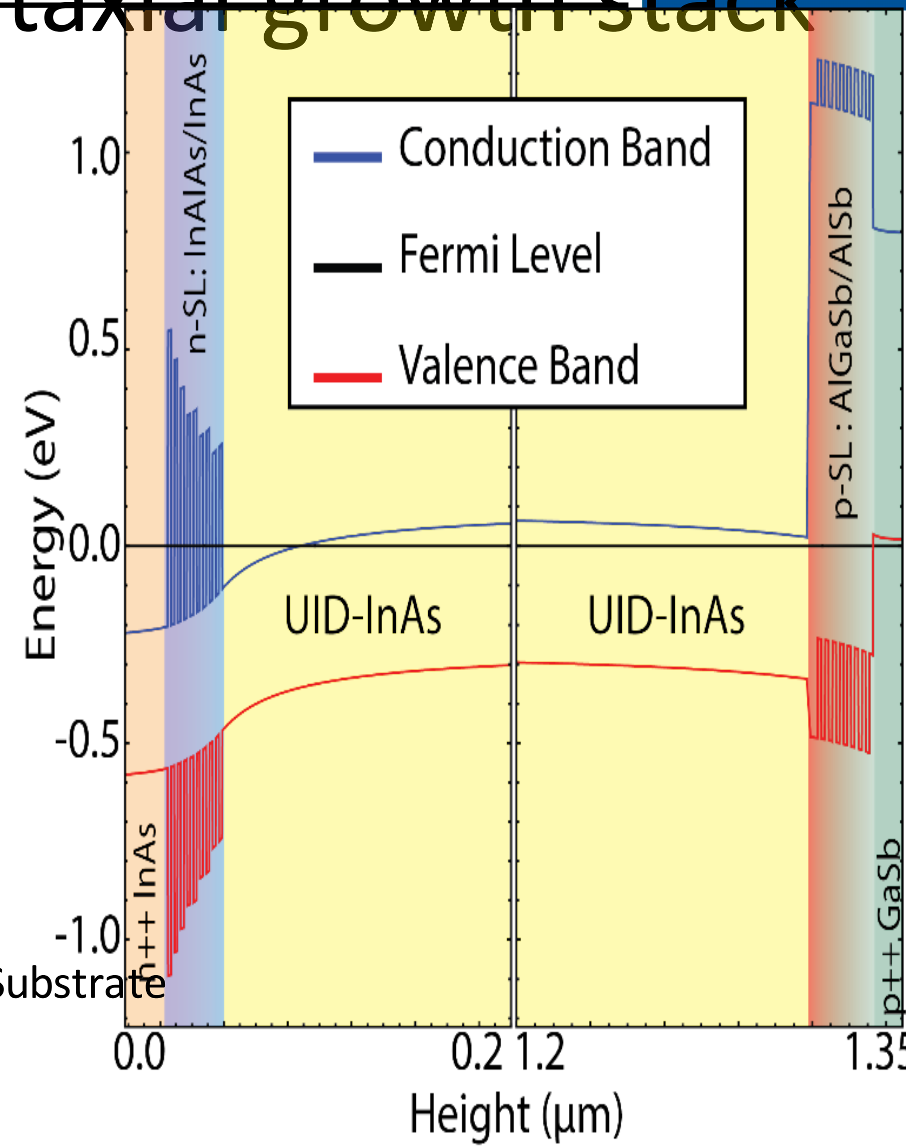

Fabrication Steps : Split-Dipole Antenna

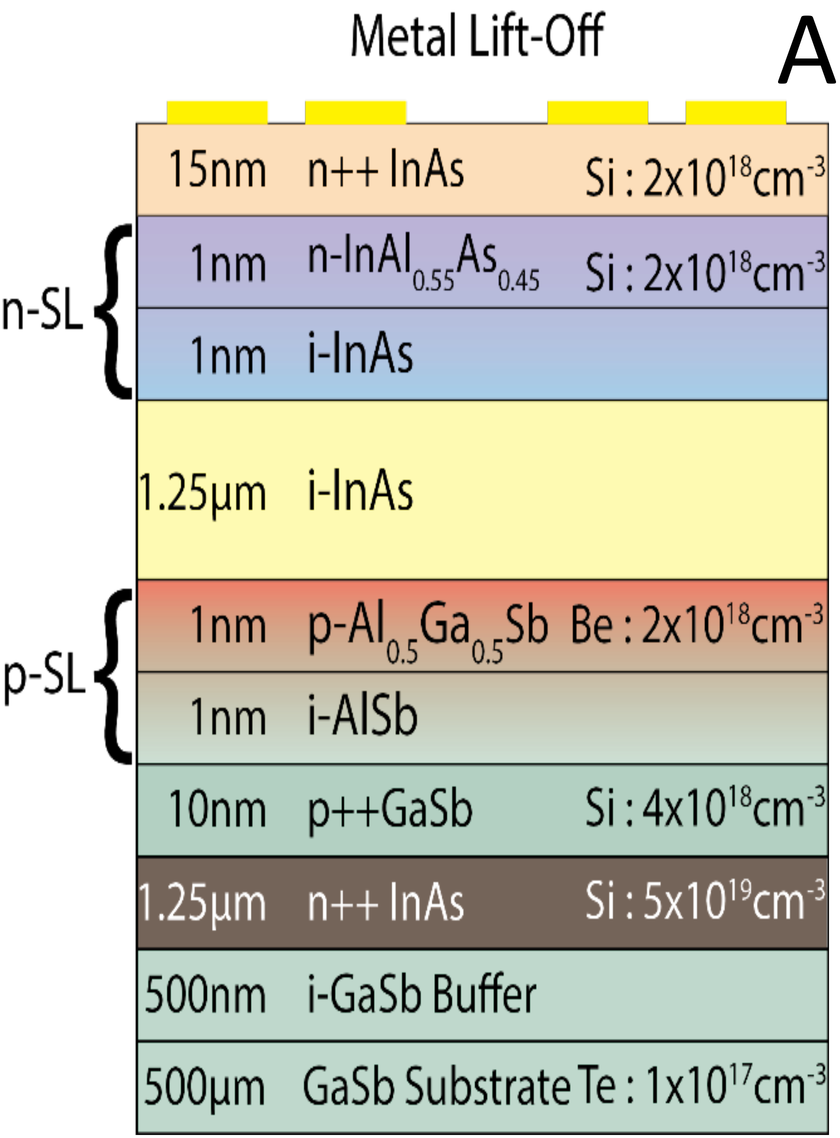

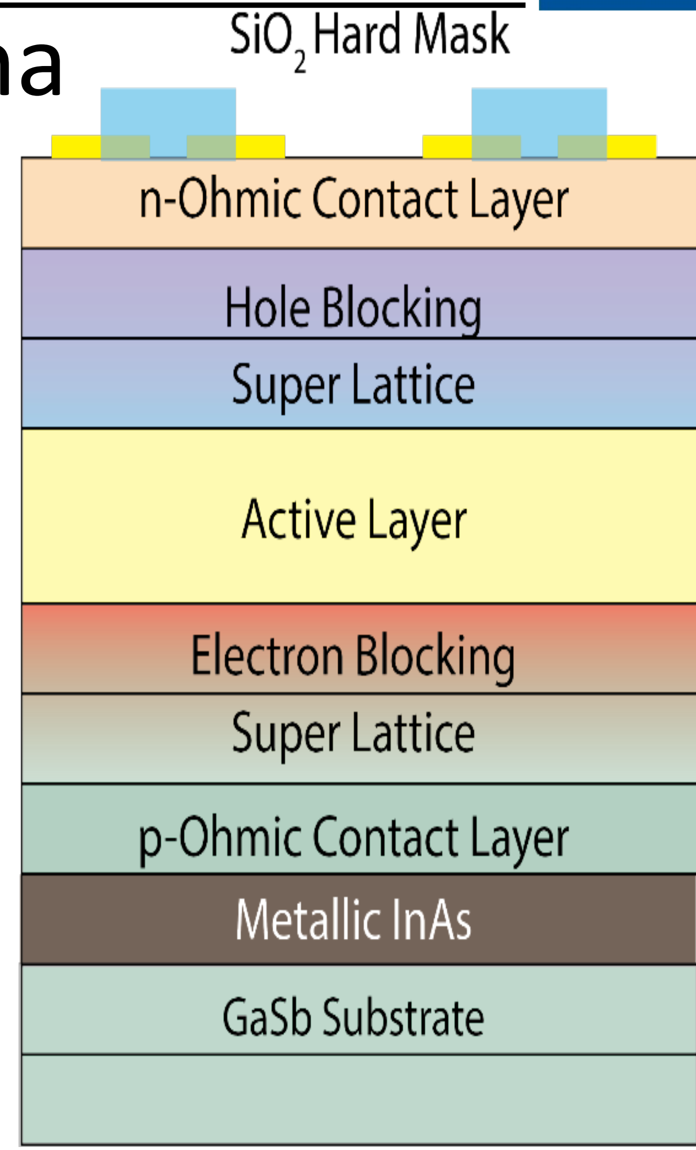

Fabrication Steps : Mesa Etch

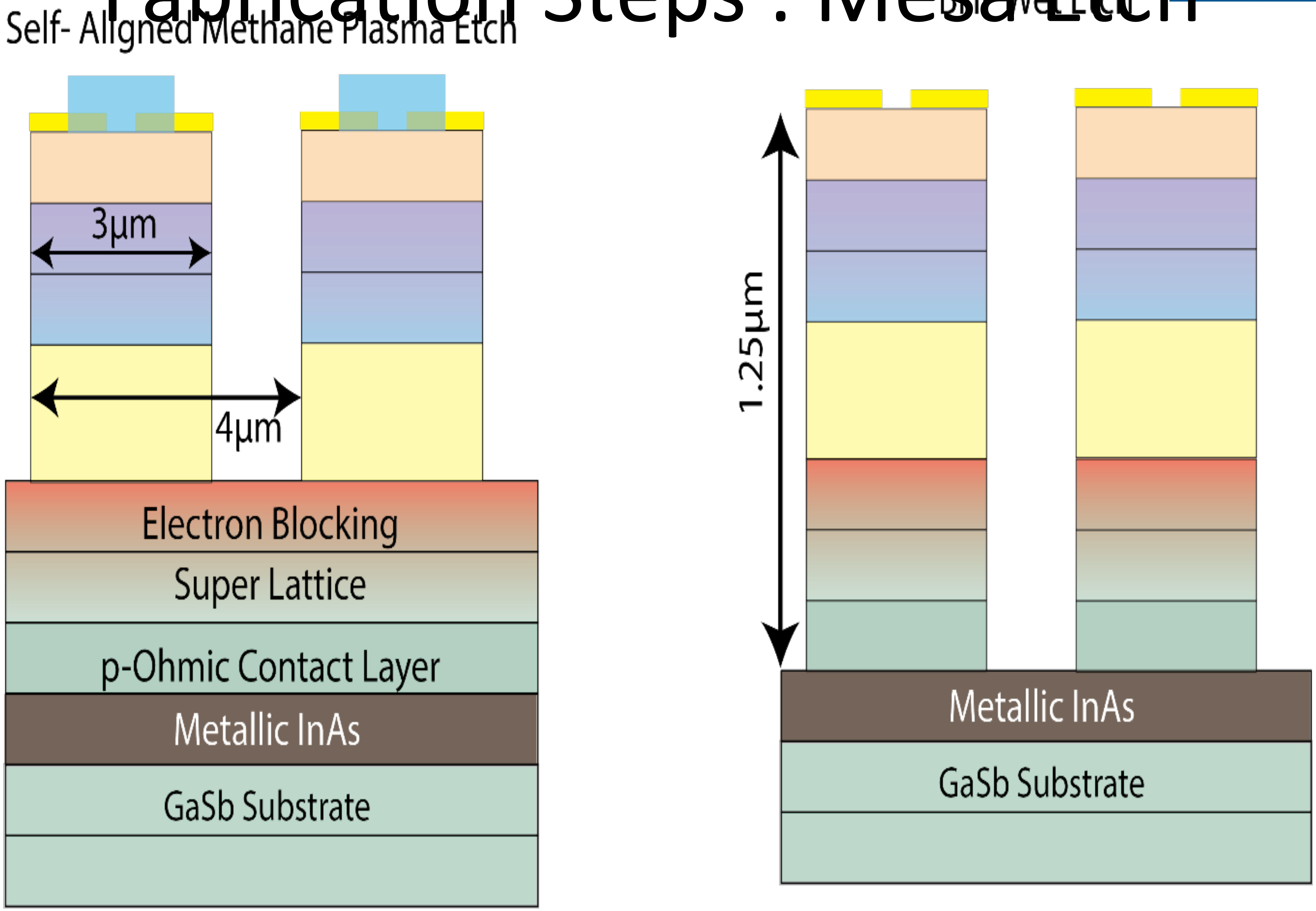

Process Flow Steps : Contact Pad

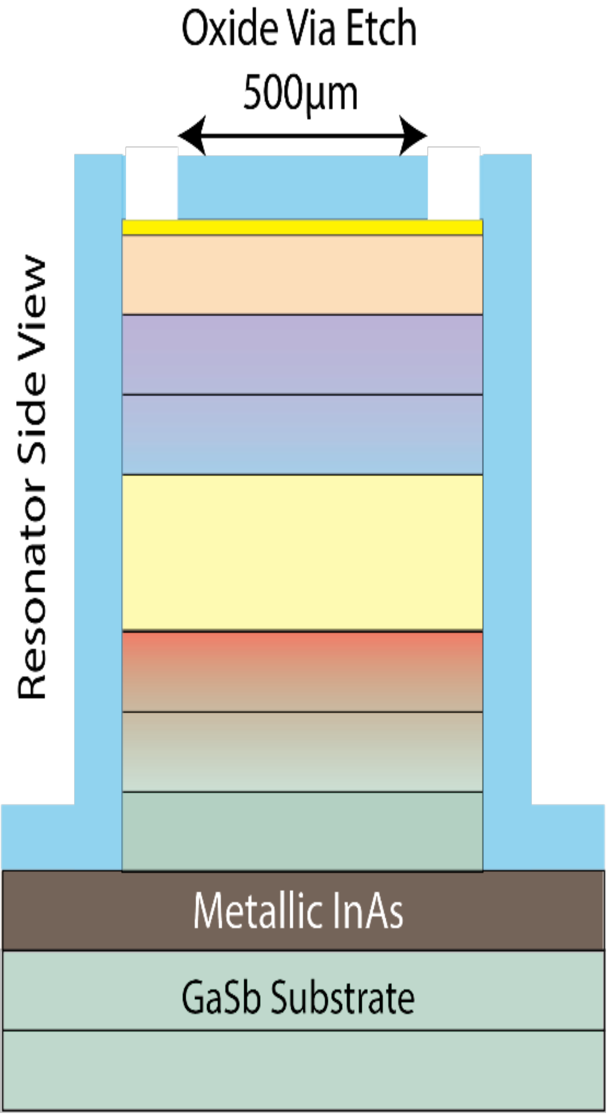

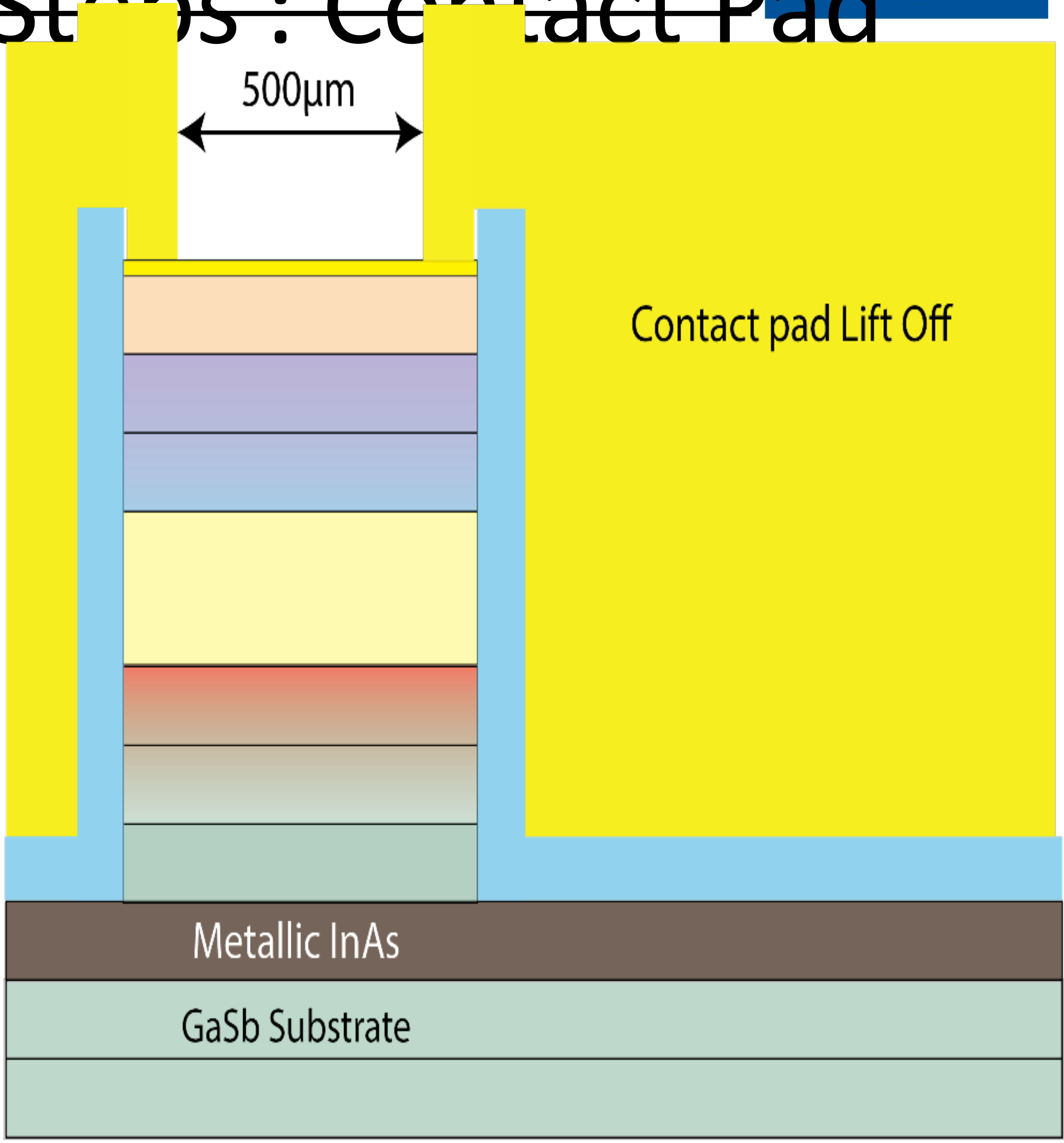

SEM Images of Self-Aligned Mesa Etch

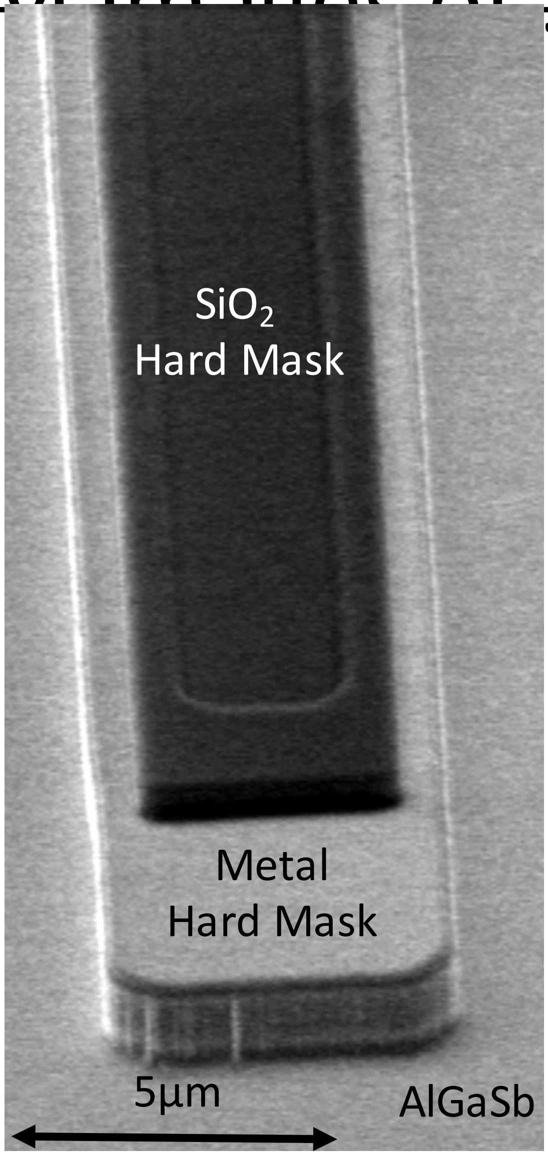

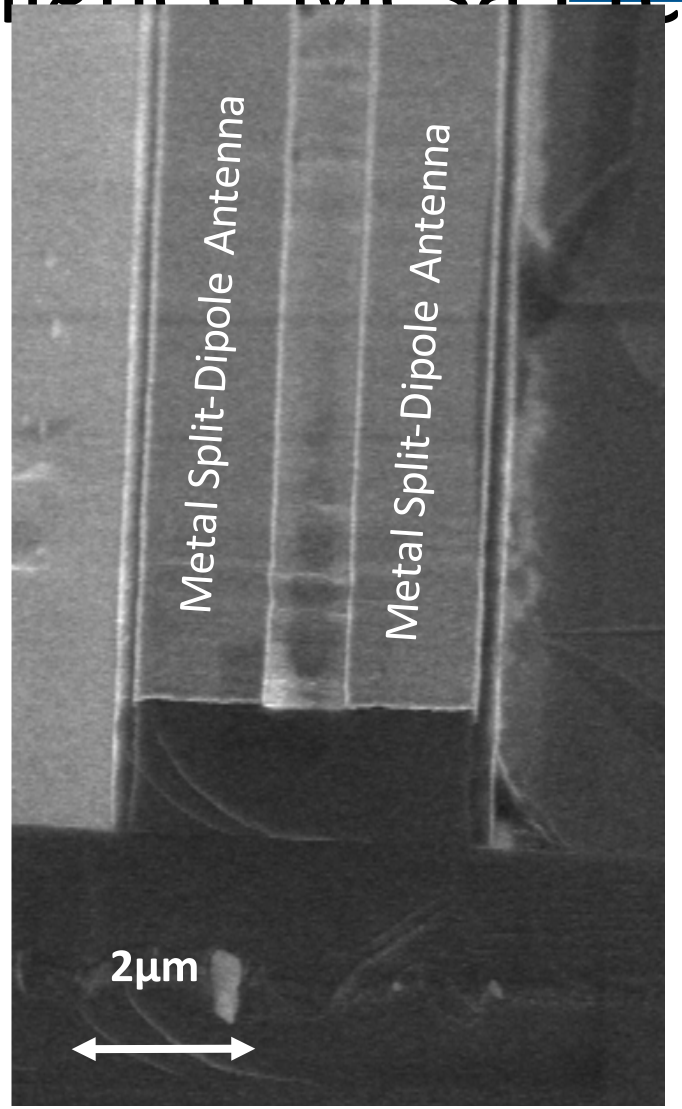

SEM Images of Side Wall Contacts

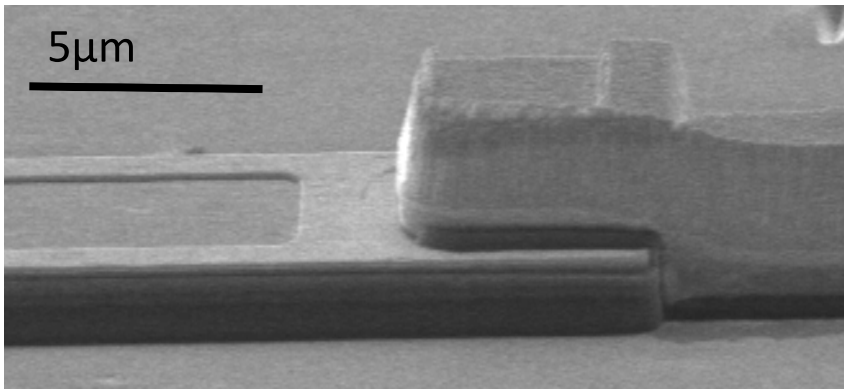

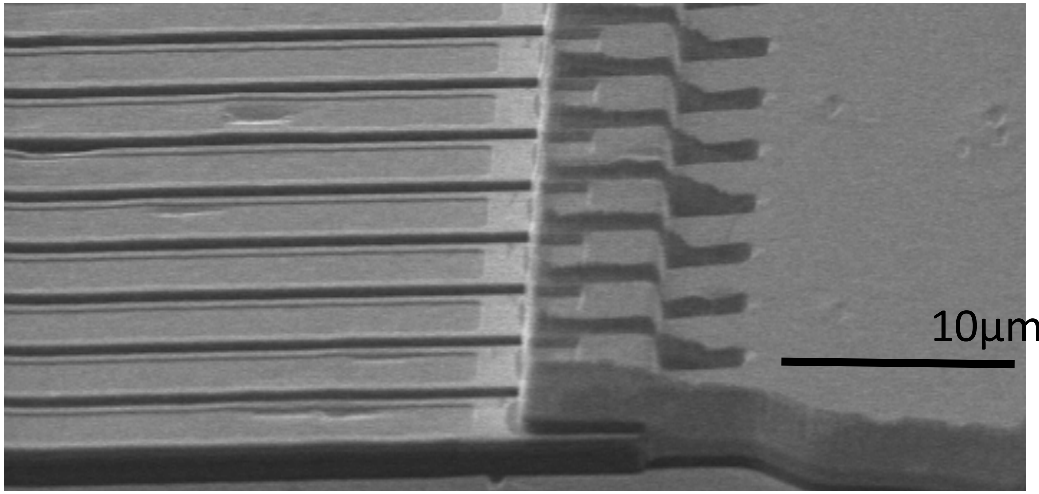

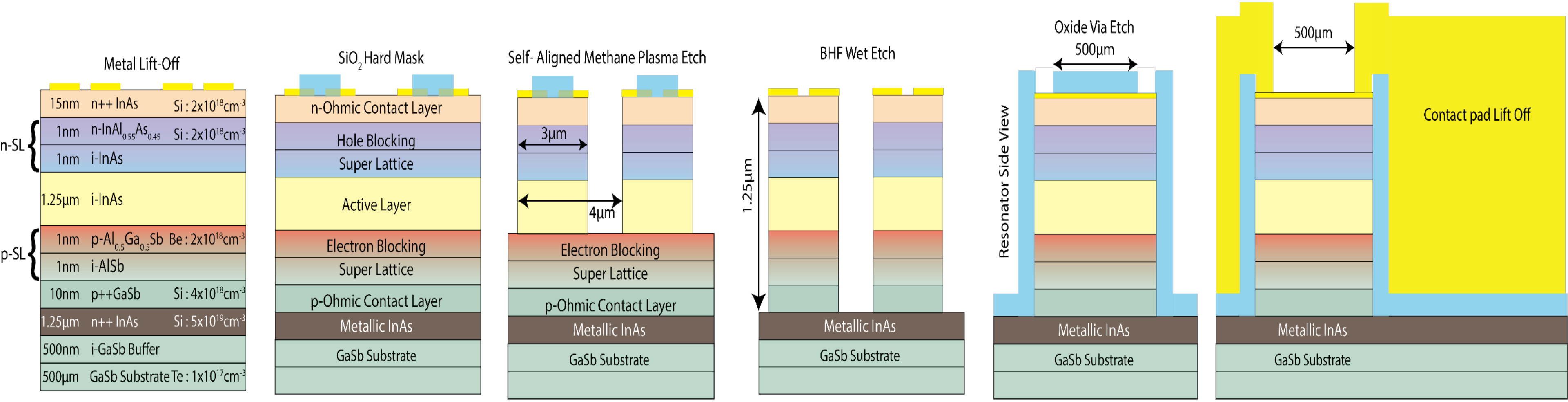

Substrate Reflectivity from Metallic InAs

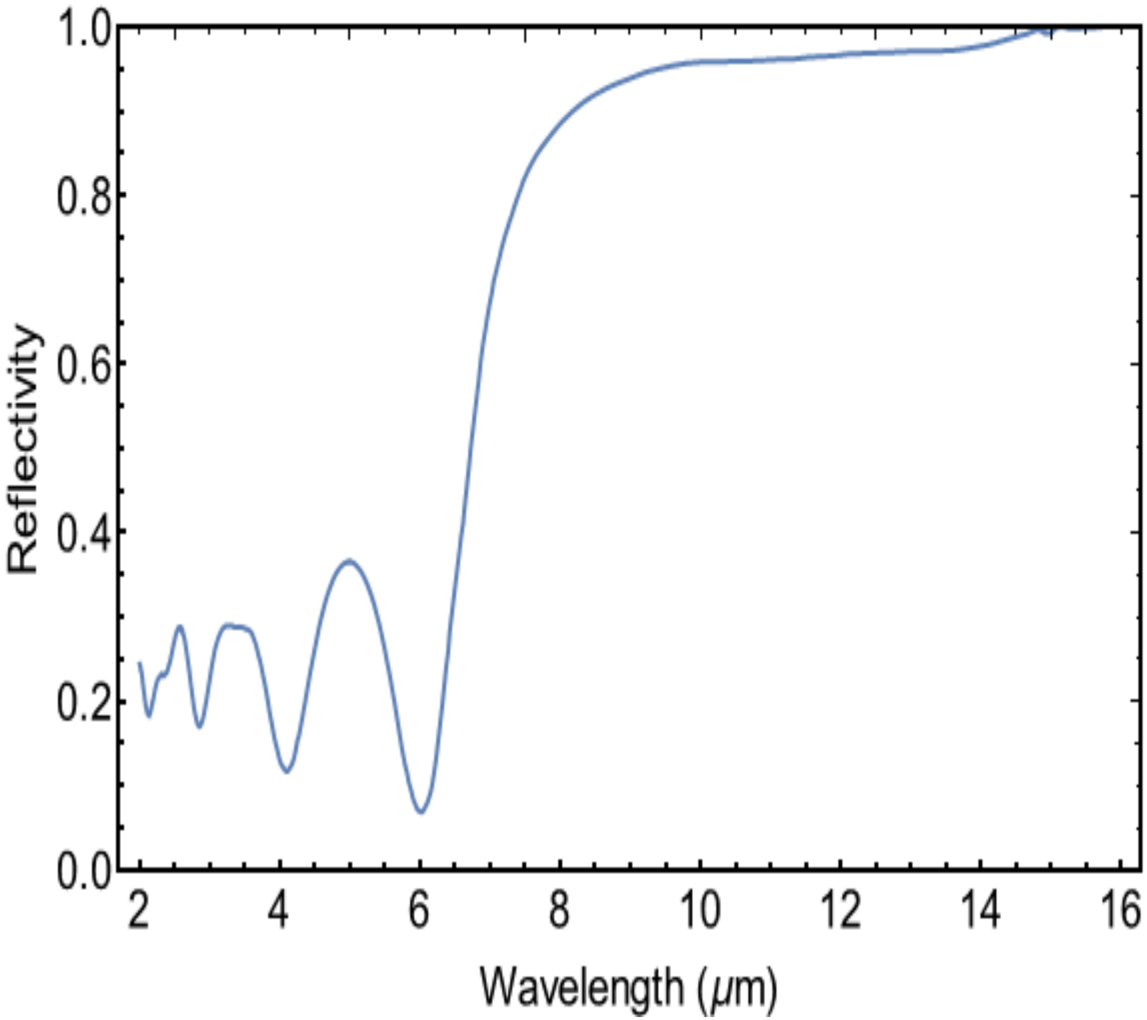

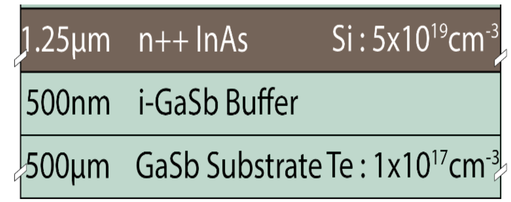

Optical Resonance tuning in forward bias

$\Delta\lambda_{res} = 200nm$

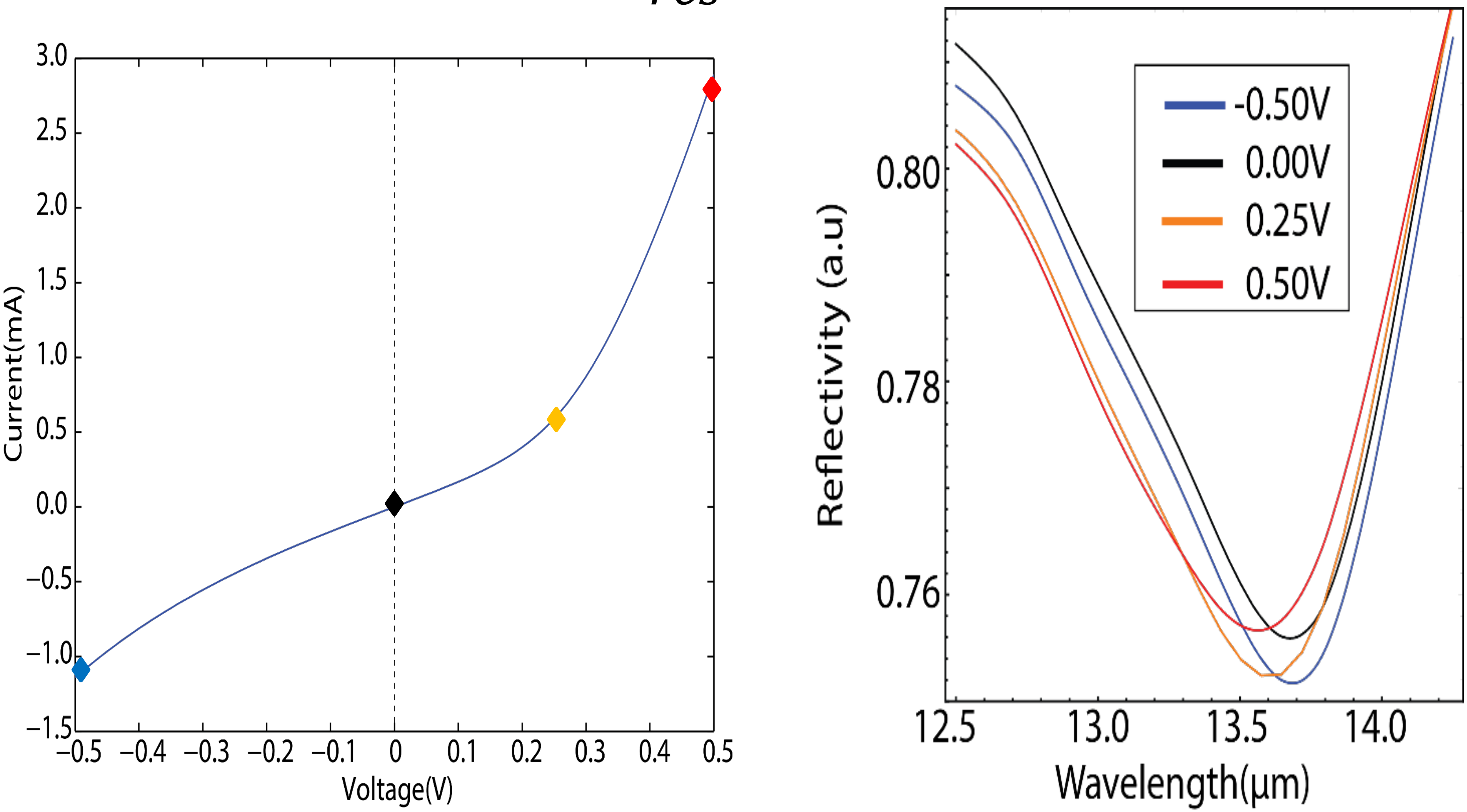

Tuning by Multiple Linewidths: Metasurface

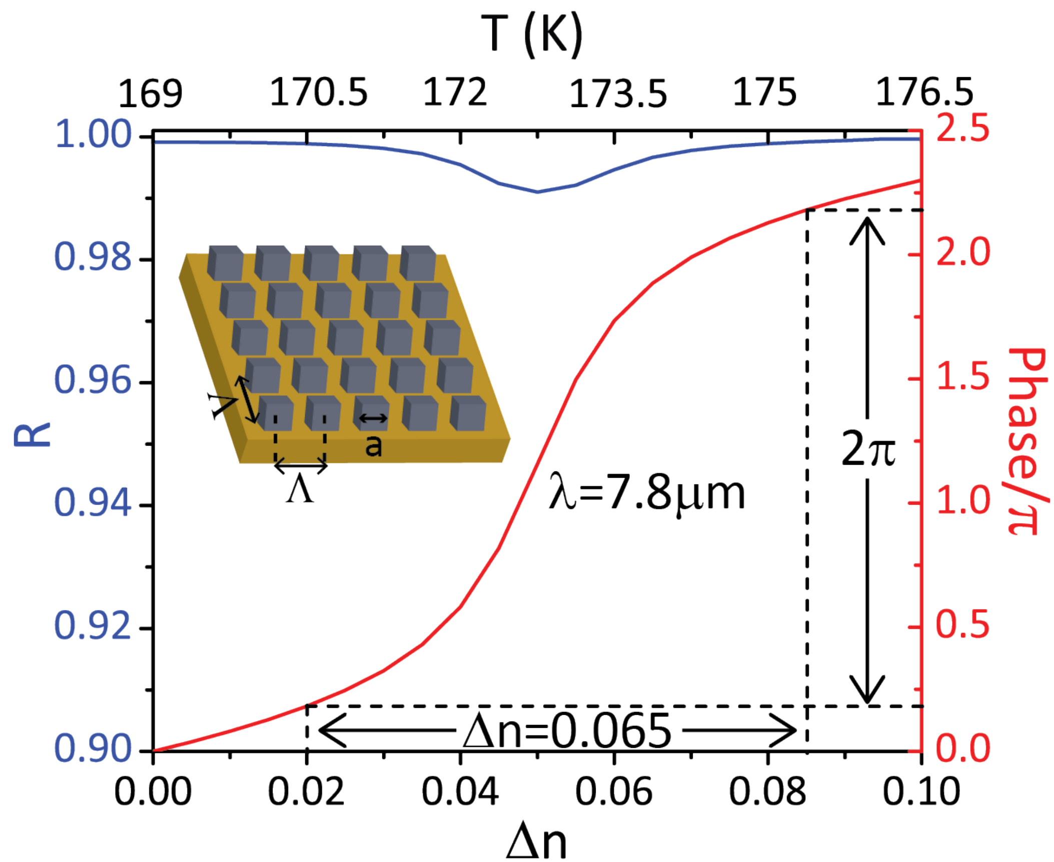

- Higher order, but still subwavelength, modes have far narrower linewidths…
- Enabling tuning by multiple linewidths for same ΔT...
- Coupled with ~ 8 fold increase in TO coefficient at low temps...
- Enables linewidth tuning with as little as 10K temperature swings!

Outline

Prasad Iyer

❶ Electrically Reconfigurable Metasurfaces (InSb)

- We theoretically demonstrate electrically reconfigurable metasurfaces with low loss and high diffraction efficiency
- We experimentally demonstrate thermo-plasmonic tuning based on both **concentration** and **mass**

Dr. Tomer Lewi

❷ Extreme Thermal Tuning of Mie Resonators (PbTe)

- PbTe is a solution processable, high refractive index semiconductor with anomalous thermo-optic tunability
- We demonstrate tuning of subwavelength resonances by more than one linewidth with less than 10 K temperature modulation

Representative Multipolar Spectrum

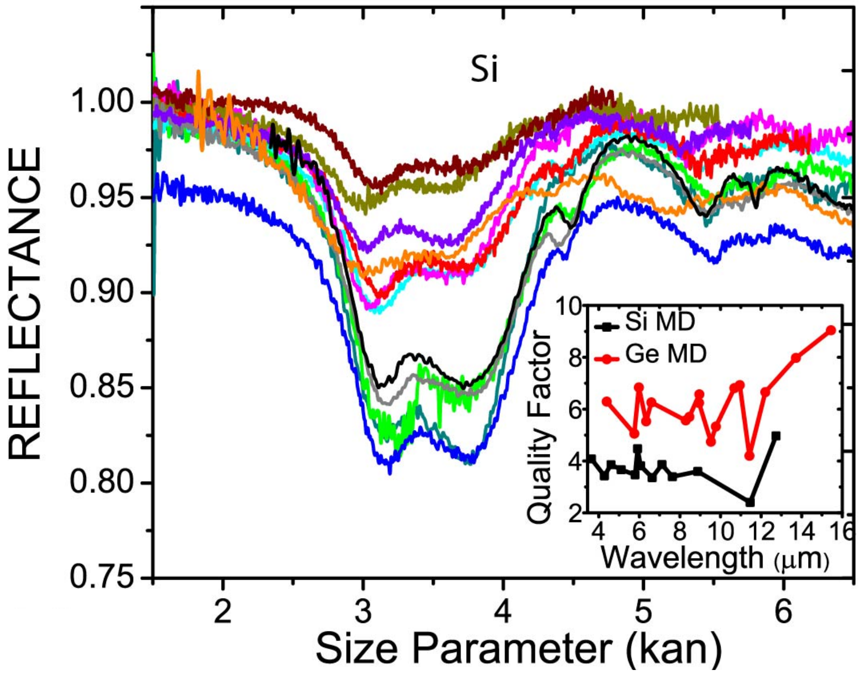

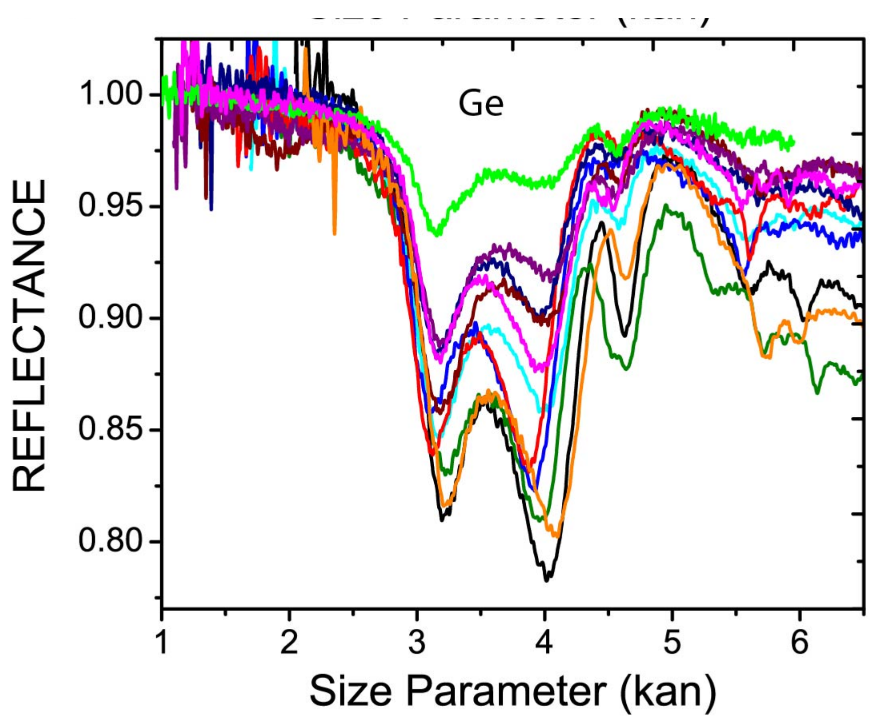

- Experimentally measure single particle extinction from reflection measurements
- Substrate induced frequency shifts are consistent w numerical simulations
- Results are consistent across order of magnitude change in size

T. Lewi, P.P.Iyer, N.A. Butakv, A. Mikhailovsky, and J.A. Schuller *Nano Lett.* **15**, 8188 (2015)

Size Dependent Mie Resonances

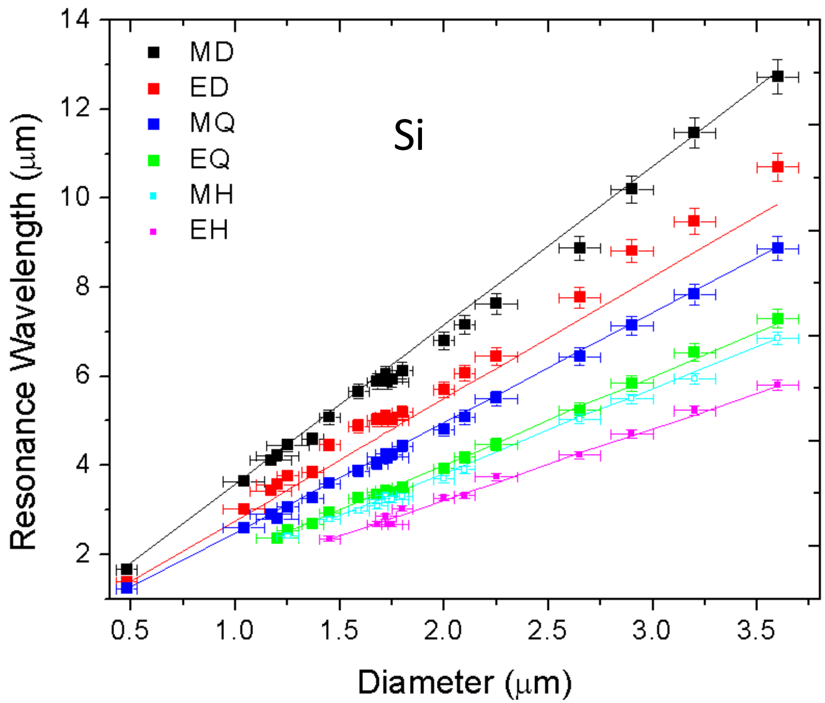

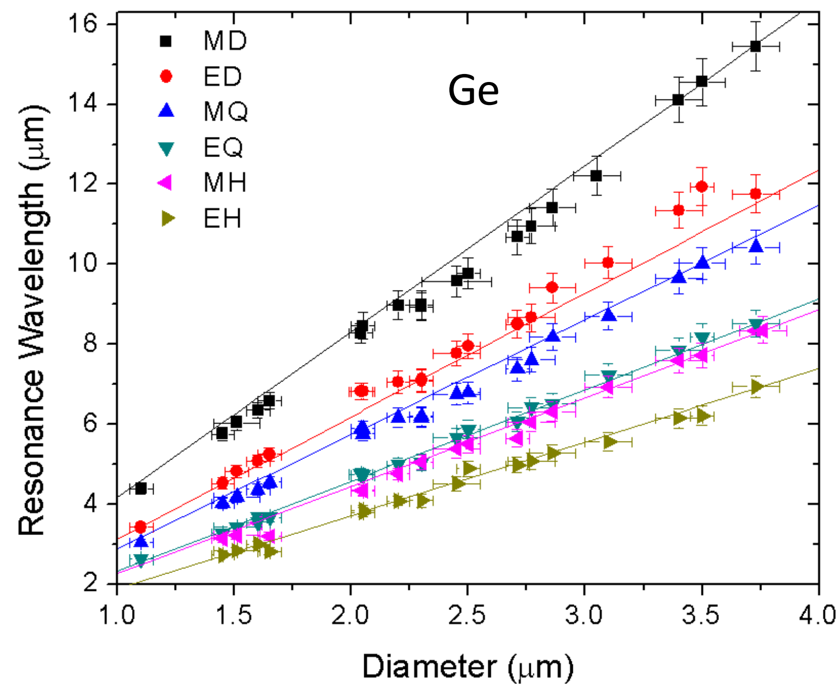

- Experimentally measure single particle extinction from reflection measurements
- Substrate induced frequency shifts are consistent w numerical simulations
- Results are consistent across order of magnitude change in size
- We reliably identify up to hexapolar modes

T. Lewi, P.P.Iyer, N.A. Butakv, A. Mikhailovsky, and J.A. Schuller *Nano Lett.* **15**, 8188 (2015)

Doping Induced Frequency Shifts

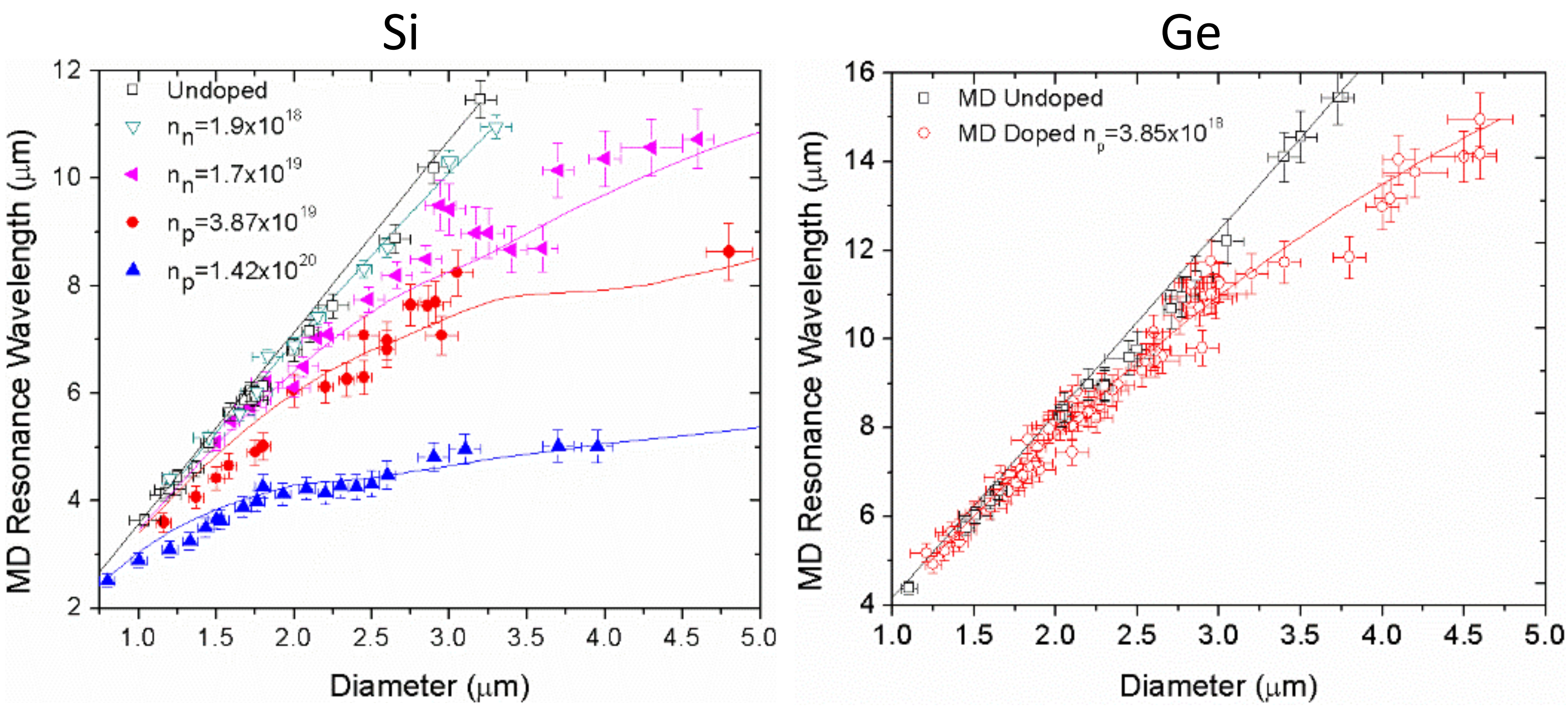

- Resonance wavelength shift increase with increase in wavelength
- Results match Drude models with ***no free parameters***
- Ge exhibits larger shifts for same doping: lower effective mass

T. Lewi, P.P.Iyer, N.A. Butakv, A. Mikhailovsky, and J.A. Schuller *Nano Lett.* **15**, 8188 (2015)

Si Free-Carrier Dispersion

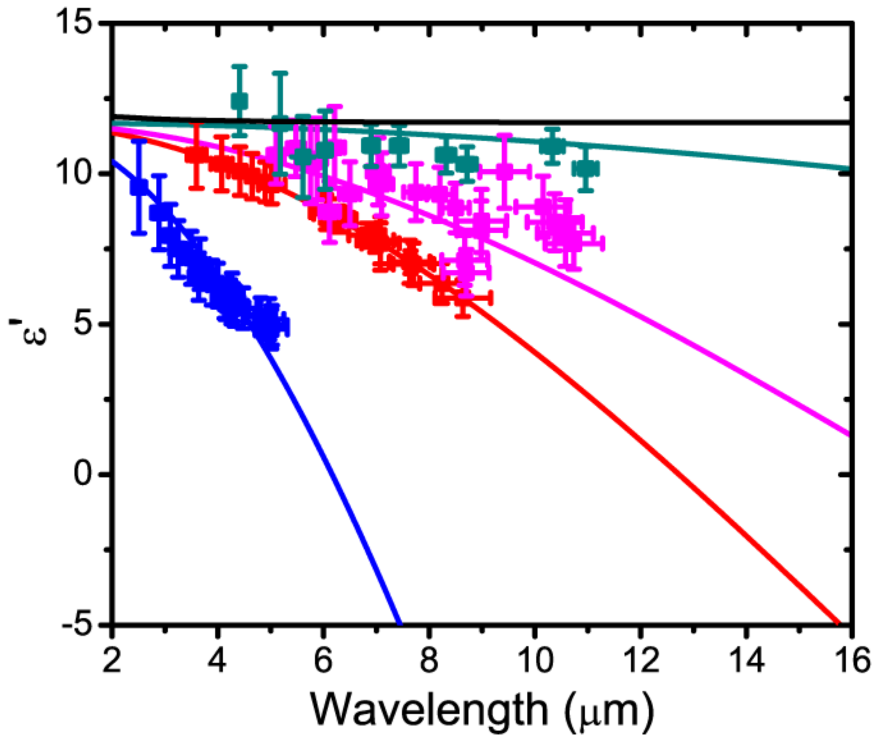

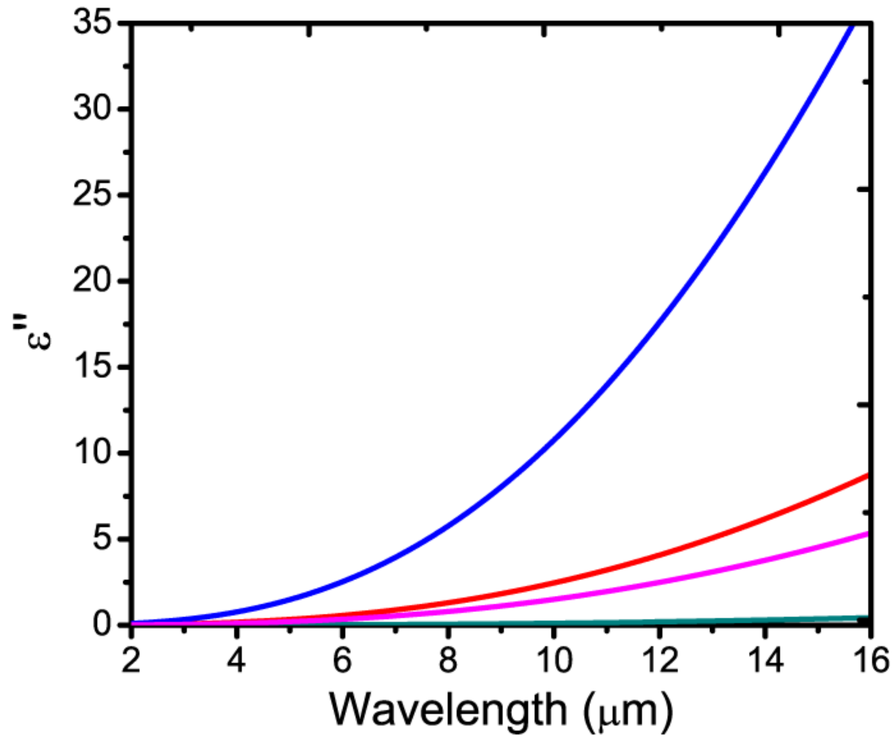

- Resonance wavelength shift increase with increase in wavelength
- Results match Drude models with ***no free parameters***
- Ge exhibits larger shifts for same doping: lower effective mass

T. Lewi, P.P.Iyer, N.A. Butakv, A. Mikhailovsky, and J.A. Schuller *Nano Lett.* **15**, 8188 (2015)

Plasmonic Modes in Highly Doped Particles

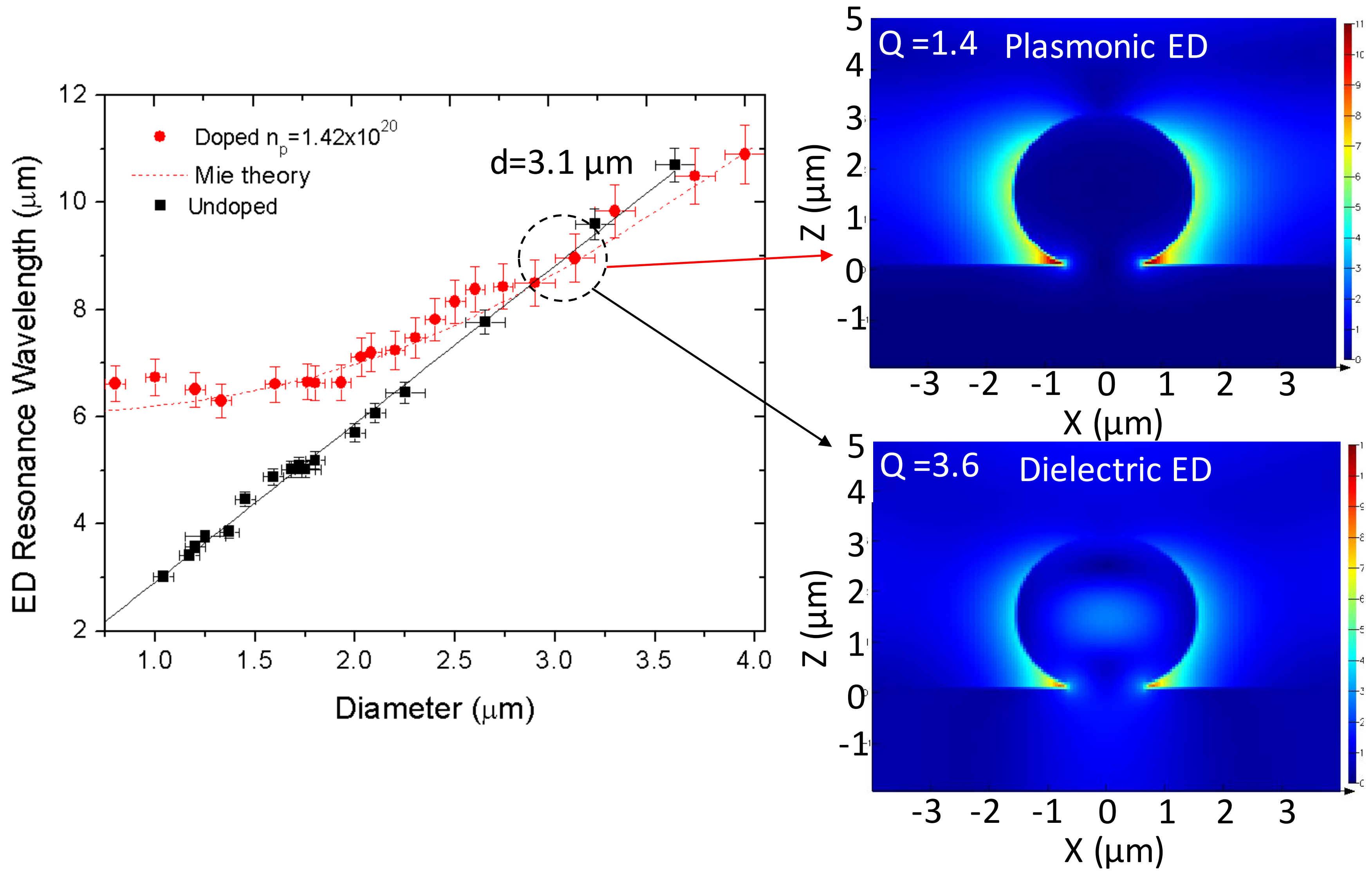

T. Lewi, P.P.Iyer, N.A. Butakv, A. Mikhailovsky, and J.A. Schuller *Nano Lett.* **15**, 8188 (2015)

Implementation: Optical Pumping

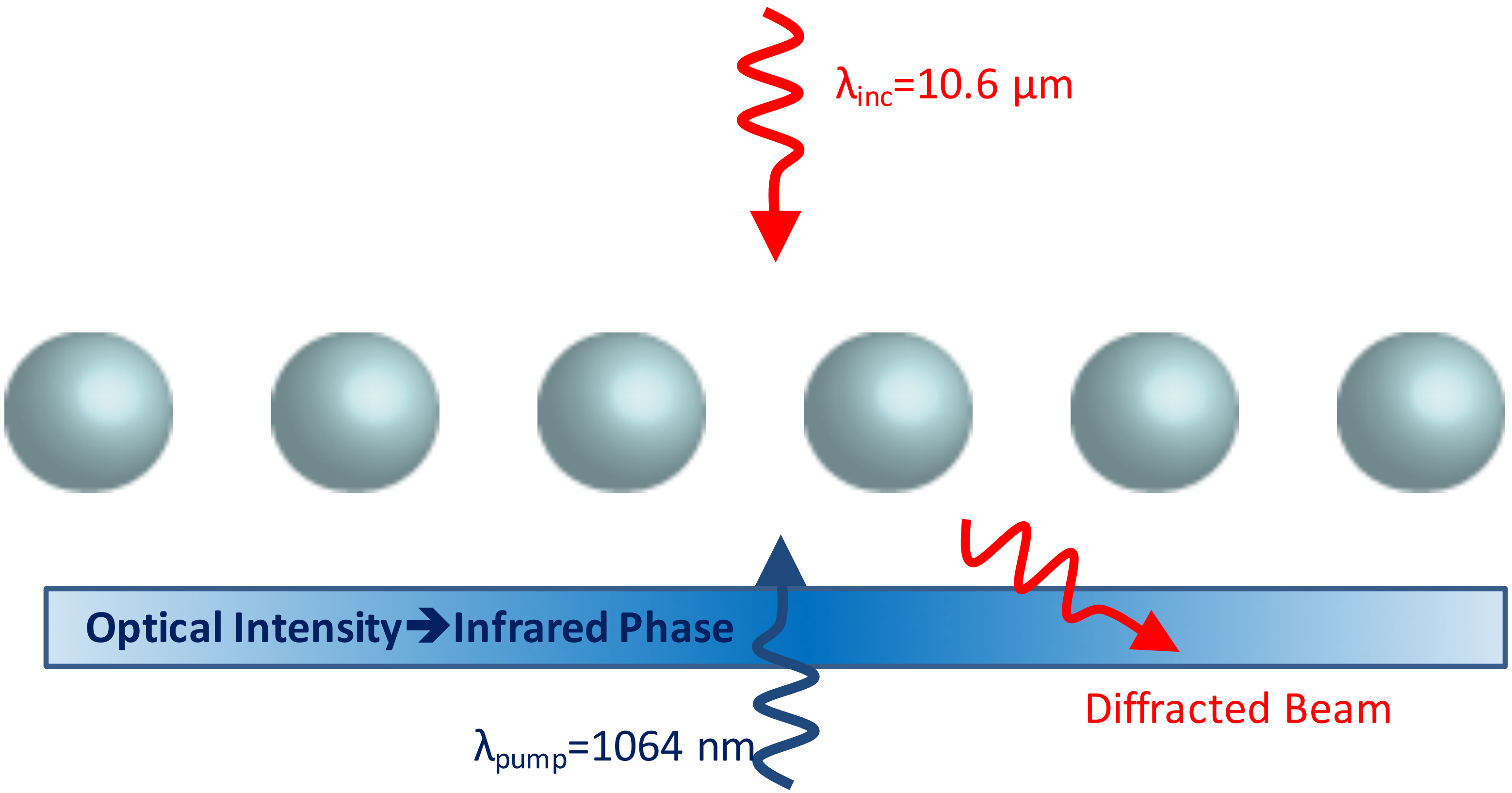

- If particles are identical, scattering is symmetric
- Symmetry can be broken by changing particle size…
- Or via optical pumping (very fast)!
- **Goal**: Generalize to arbitrary phase patterns

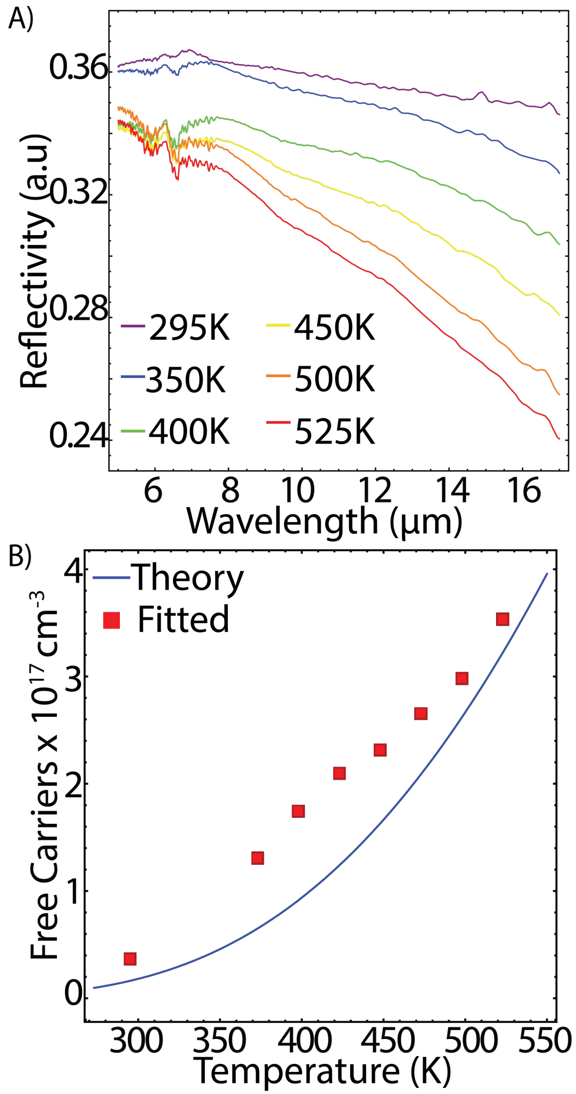
A)
0.36
0.32
0.28
0.24
Reflectivity (a.u)
295K
350K
400K
450K
500K
525K
6
8
10
12
14
16
Wavelength (μm)
B)
Theory
Fitted
4
3
2
1
0
Free Carriers x 10^17 cm^-3
300
350
400
450
500
550
Temperature (K)

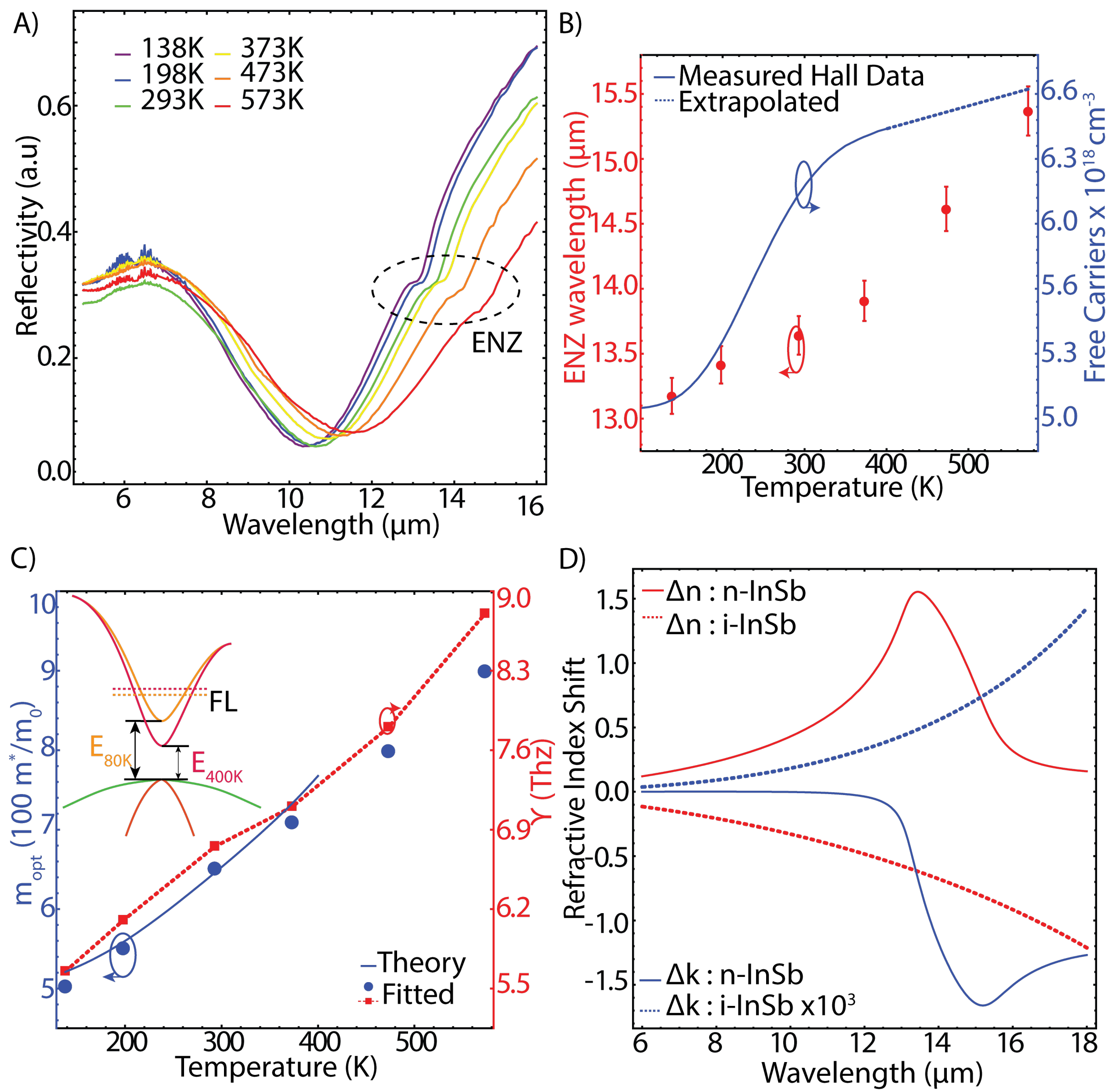
A)
138K
198K
293K
373K
473K
573K
Reflectivity (a.u)
Wavelength (µm)
ENZ
B)
Measured Hall Data
Extrapolated
ENZ wavelength (µm)
Free Carriers x 10^{18} cm^{-3}
Temperature (K)
C)
m_{opt} (100 m^*/m_0)
γ (Thz)
FL
E_{80K}
E_{400K}
Theory
Fitted
Temperature (K)
D)
Δn : n-InSb
Δn : i-InSb
Δk : n-InSb
Δk : i-InSb x10^3
Refractive Index Shift
Wavelength (µm)

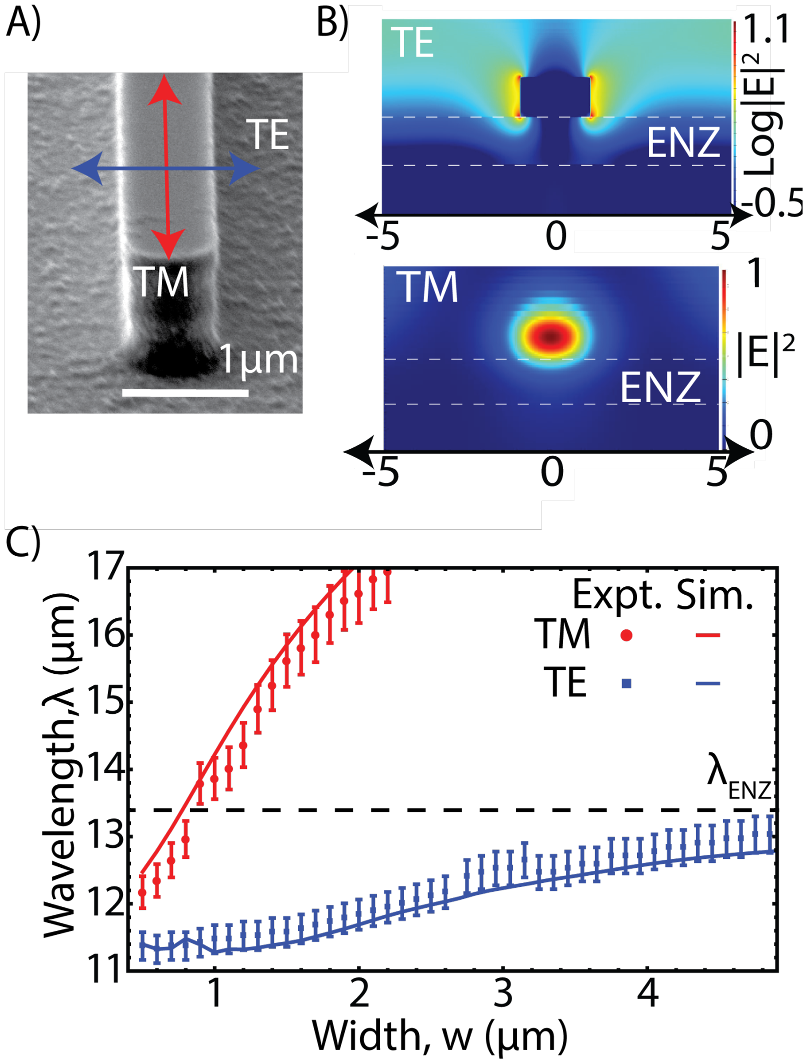

A)
TE
TM
1µm
B)
TE
ENZ
1.1
Log|E|²
-0.5
-5
0
5
TM
ENZ
1
|E|²
0
-5
0
5
C)
Expt. Sim.
TM
TE
λENZ
Wavelength,λ (µm)
17
16
15
14
13
12
11
1
2
3
4
Width, w (µm)

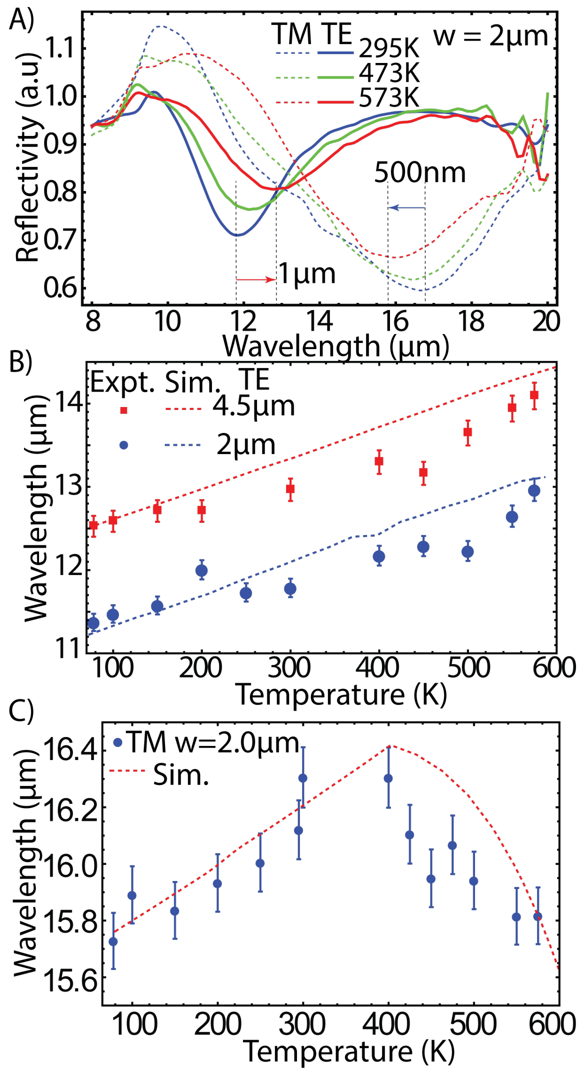
A)
TM TE
295K
473K
573K
w = 2μm
500nm
1μm
Reflectivity (a.u)
Wavelength (μm)
B)
Expt. Sim. TE
4.5μm
2μm
Wavelength (μm)
Temperature (K)
C)
TM w=2.0μm
Sim.
Wavelength (μm)
Temperature (K)

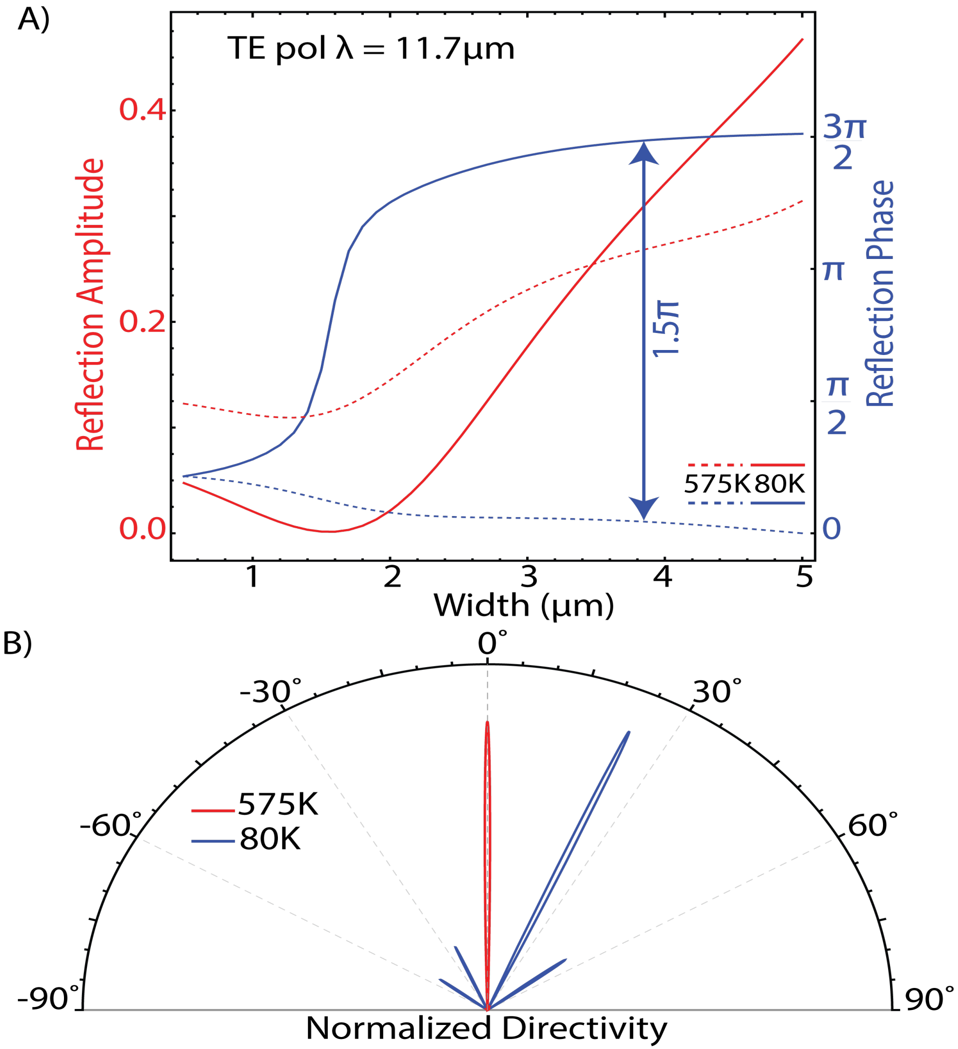
A)
TE pol λ = 11.7μm
Reflection Amplitude
0.4
0.2
0.0
3π
2
π
π
2
0
Reflection Phase
1.5π
575K
80K
1
2
3
4
5
Width (μm)
B)
0˚
-30˚
30˚
-60˚
60˚
-90˚
90˚
575K
80K
Normalized Directivity

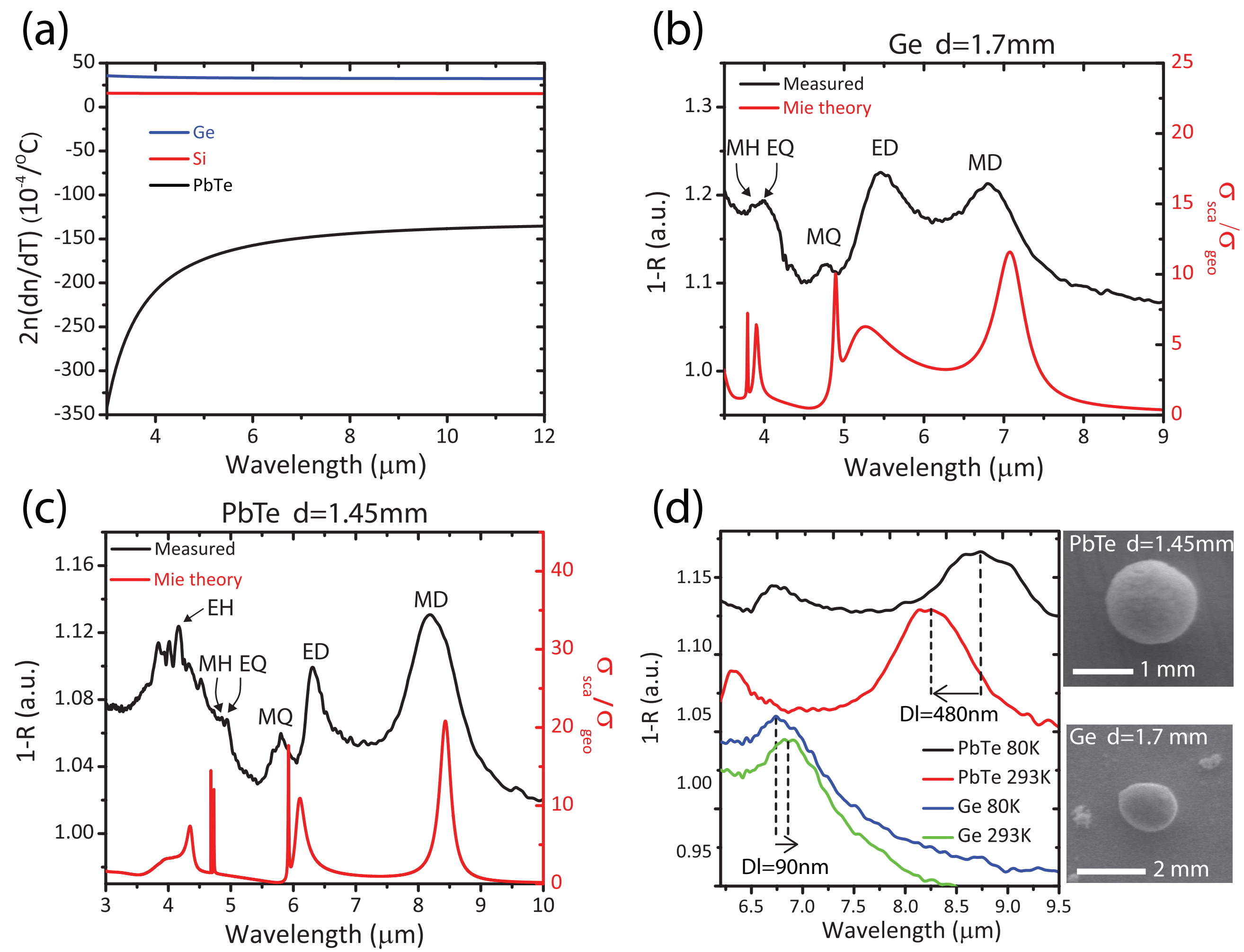
(a)
2n(dn/dT) (10⁻⁴/°C)
Ge
Si
PbTe
Wavelength (μm)
(b)
Ge d=1.7mm
Measured
Mie theory
MH EQ
ED
MD
MQ
1-R (a.u.)
σsca/σgeo
Wavelength (μm)
(c)
PbTe d=1.45mm
Measured
Mie theory
EH
MH EQ
ED
MD
MQ
1-R (a.u.)
σsca/σgeo
Wavelength (μm)
(d)
Dl=480nm
Dl=90nm
PbTe 80K
PbTe 293K
Ge 80K
Ge 293K
1-R (a.u.)
Wavelength (μm)
PbTe d=1.45mm
1 mm
Ge d=1.7 mm
2 mm

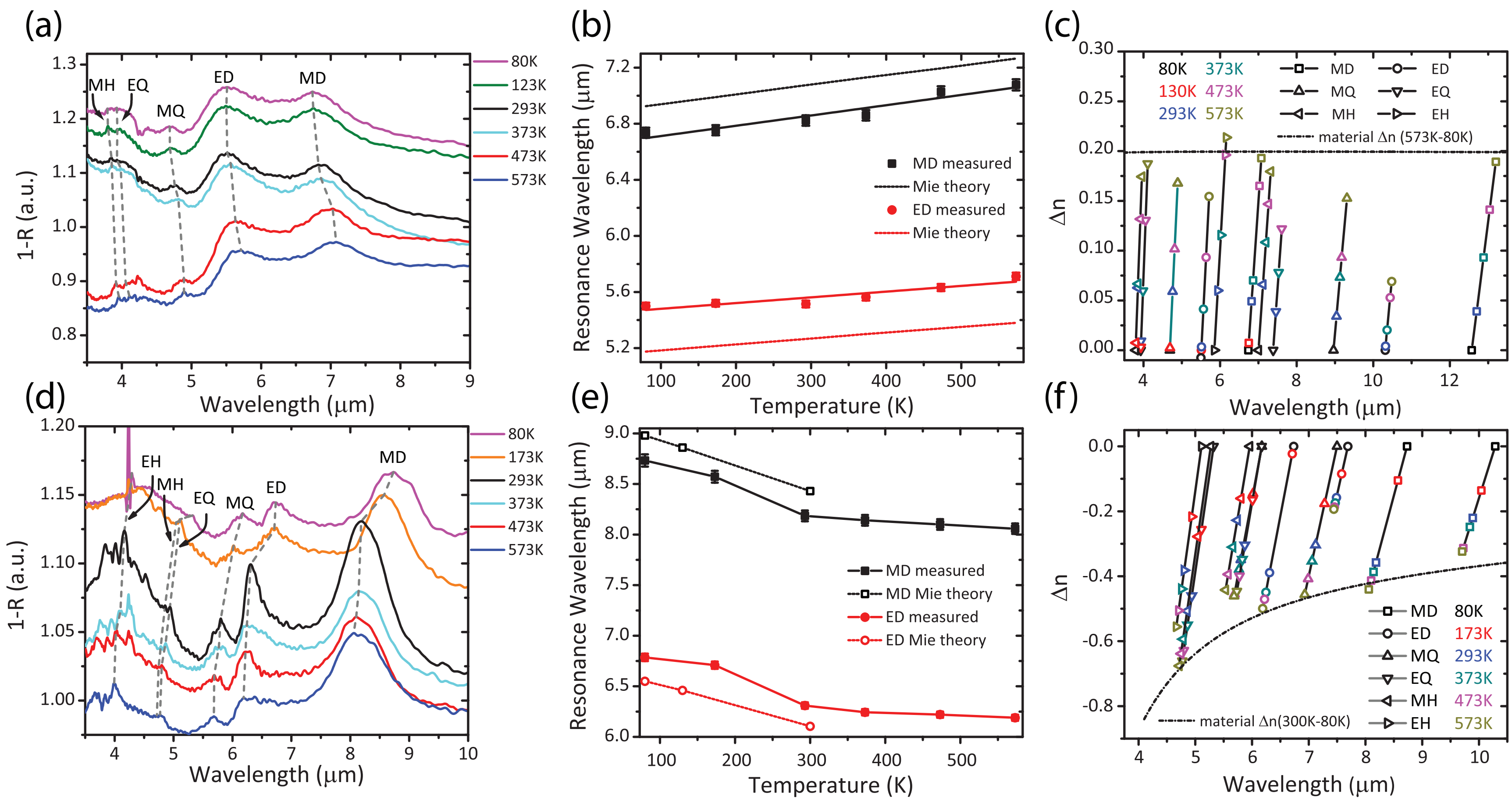
(a)
1-R (a.u.)
Wavelength (μm)
MH
EQ
MQ
ED
MD
80K
123K
293K
373K
473K
573K
(b)
Resonance Wavelength (μm)
Temperature (K)
MD measured
Mie theory
ED measured
Mie theory
(c)
Δn
Wavelength (μm)
80K 373K
130K 473K
293K 573K
MD ED
MQ EQ
MH EH
material Δn (573K-80K)
(d)
1-R (a.u.)
Wavelength (μm)
EH
MH
EQ
MQ
ED
MD
80K
173K
293K
373K
473K
573K
(e)
Resonance Wavelength (μm)
Temperature (K)
MD measured
MD Mie theory
ED measured
ED Mie theory
(f)
Δn
Wavelength (μm)
MD 80K
ED 173K
MQ 293K
EQ 373K
MH 473K
EH 573K
material Δn(300K-80K)

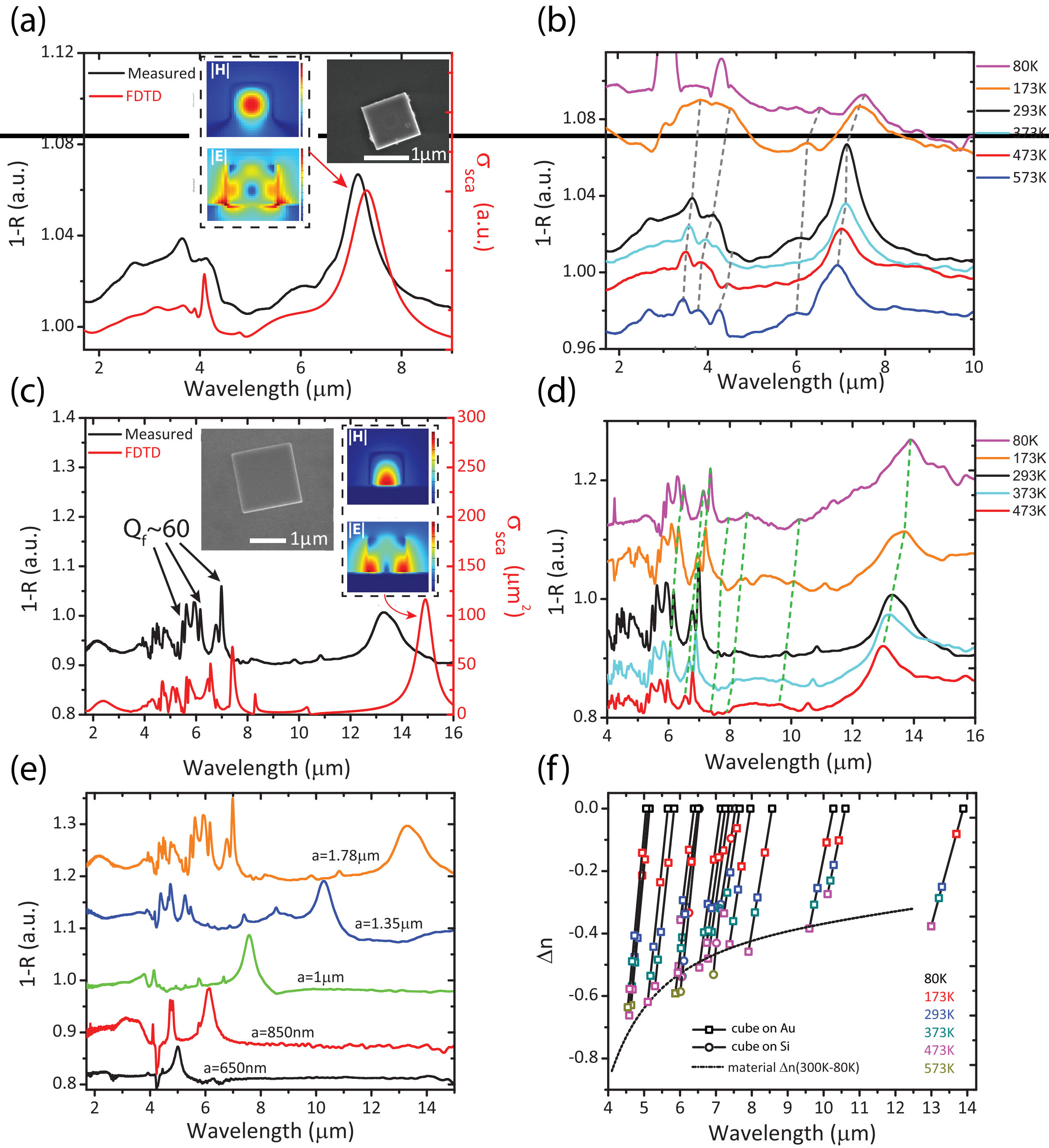
(a)
Measured
FDTD
|H|
|E|
1µm
1-R (a.u.)
σ sca (a.u.)
Wavelength (µm)
(b)
80K
173K
293K
473K
573K
1-R (a.u.)
Wavelength (µm)
(c)
Measured
FDTD
Q f ~60
1µm
|H|
|E|
1-R (a.u.)
σ sca (µm²)
Wavelength (µm)
(d)
80K
173K
293K
373K
473K
1-R (a.u.)
Wavelength (µm)
(e)
a=1.78µm
a=1.35µm
a=1µm
a=850nm
a=650nm
1-R (a.u.)
Wavelength (µm)
(f)
Δn
cube on Au
cube on Si
material Δn(300K-80K)
80K
173K
293K
373K
473K
573K
Wavelength (µm)

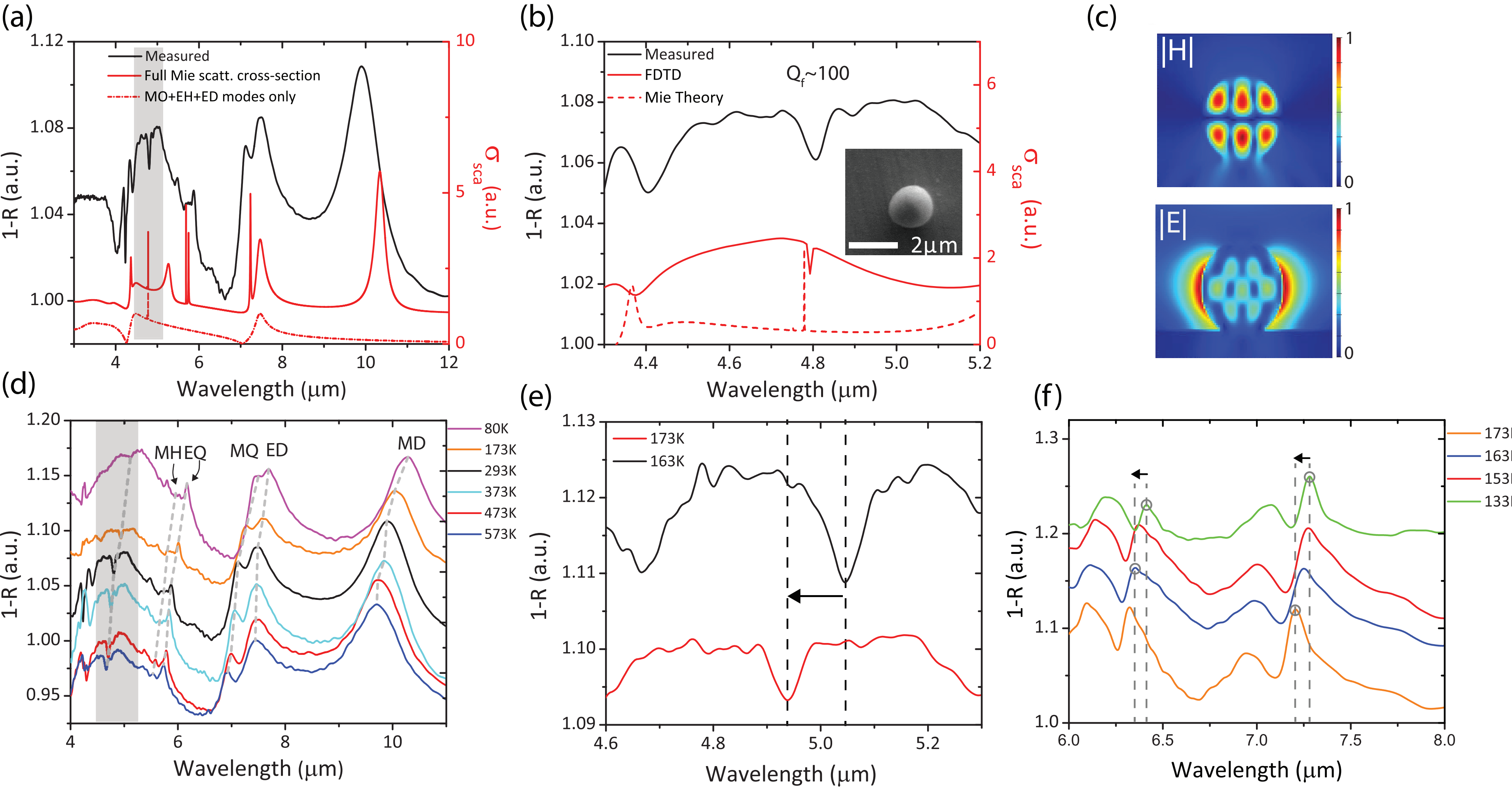
(a)
Measured
Full Mie scatt. cross-section
MO+EH+ED modes only
1-R (a.u.)
σ_{sca} (a.u.)
Wavelength (μm)
(b)
Measured
FDTD
Mie Theory
Q_f~100
2μm
1-R (a.u.)
σ_{sca} (a.u.)
Wavelength (μm)
(c)
|H|
|E|
(d)
MHEQ
MQ ED
MD
80K
173K
293K
373K
473K
573K
1-R (a.u.)
Wavelength (μm)
(e)
173K
163K
1-R (a.u.)
Wavelength (μm)
(f)
173K
163K
153K
133K
1-R (a.u.)
Wavelength (μm)

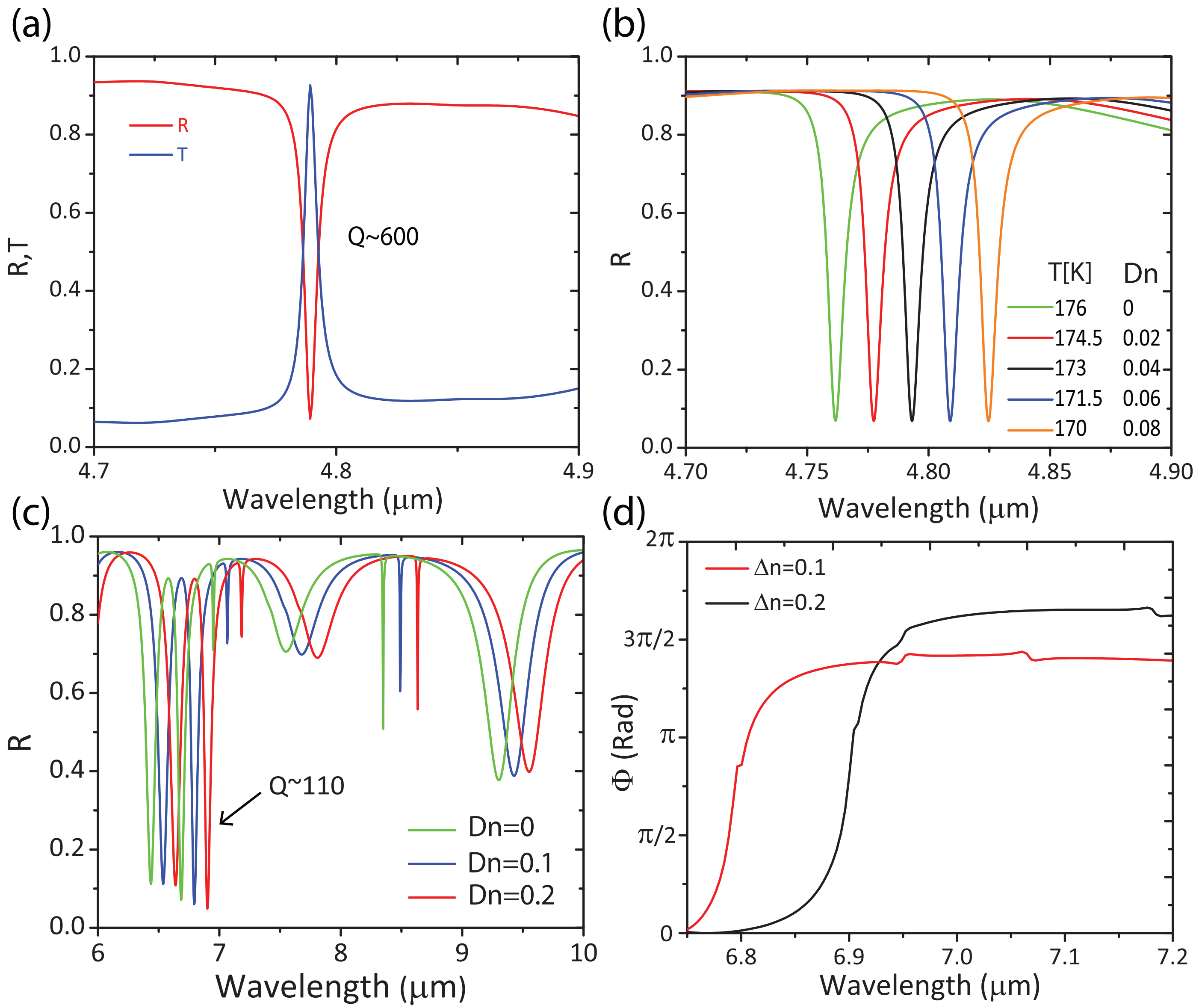
(a)
R
T
Q~600
R,T
Wavelength (μm)
(b)
R
T[K] Dn
176 0
174.5 0.02
173 0.04
171.5 0.06
170 0.08
Wavelength (μm)
(c)
Q~110
Dn=0
Dn=0.1
Dn=0.2
R
Wavelength (μm)
(d)
Δn=0.1
Δn=0.2
Φ (Rad)
Wavelength (μm)

Induced index shift

PbTe

spheres

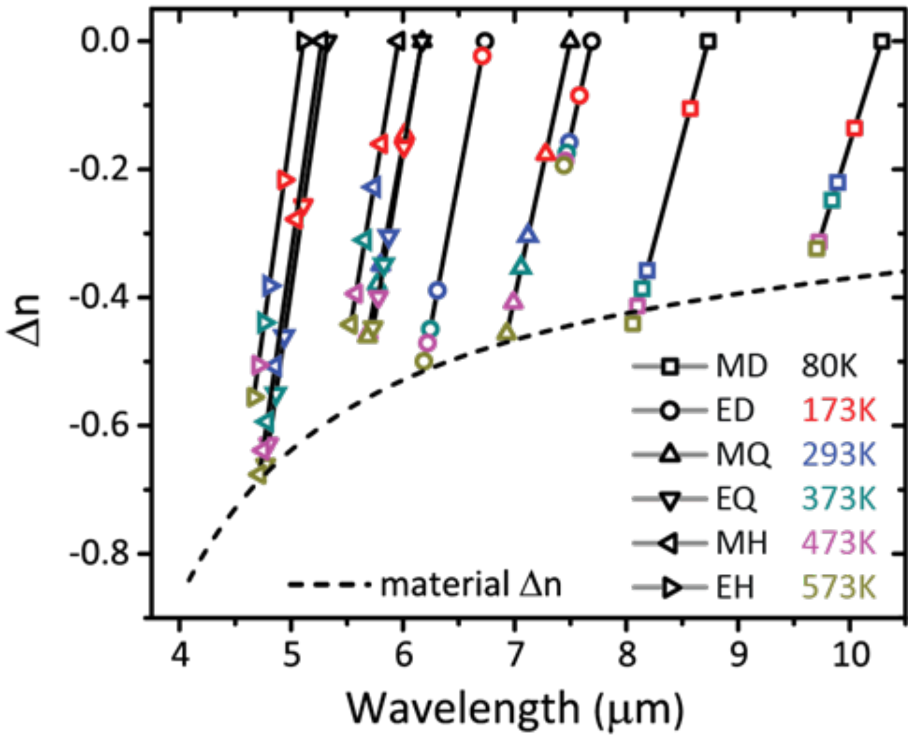

cubes

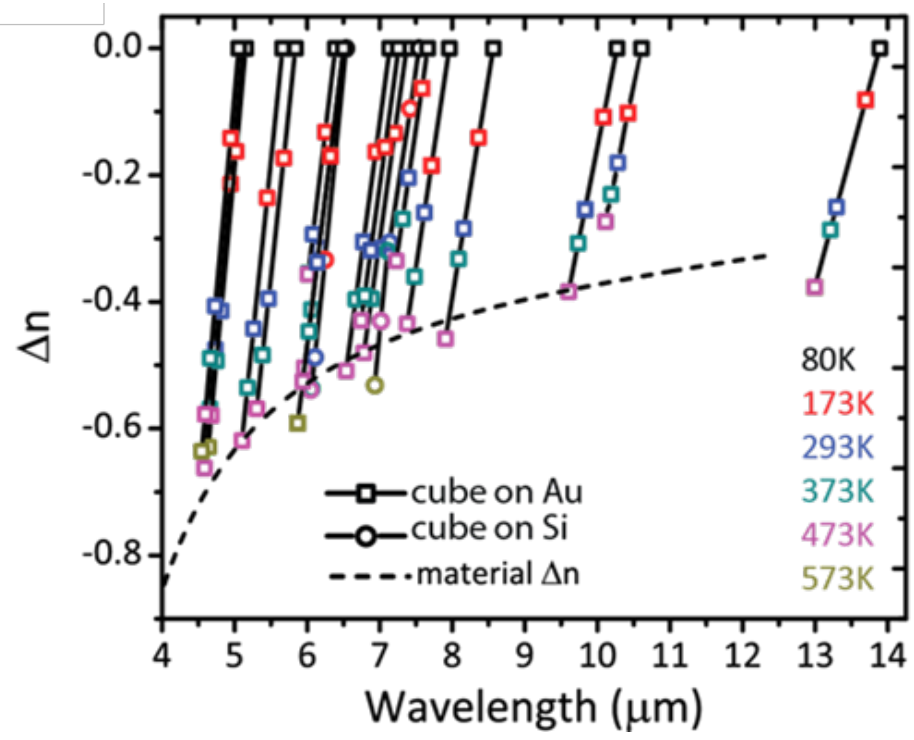

Thermo-optic tuning of semiconductors

Thermo-optic coefficient:

Thermal expansion (usually <0 and small) and Bandgap (usually >0 and larger) terms:

$$2n\frac{dn}{dT} = (n_\infty^2 - 1)\left(-3\alpha R - \frac{1}{E_g}\frac{dE_g}{dT}R^2\right); \quad R = \frac{\lambda^2}{\lambda^2 - \lambda_{ig}^2}$$

Thermal expansion: $-3\alpha R$ — usually <0 and small

Bandgap: $-\frac{1}{E_g}\frac{dE_g}{dT}R^2$ — usually >0 and larger

in most materials $\frac{dn}{dT} > 0$

TEM of PbTe cubes

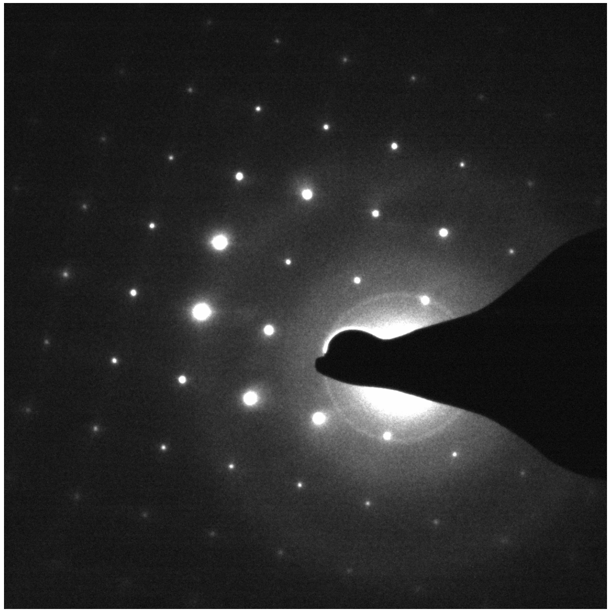

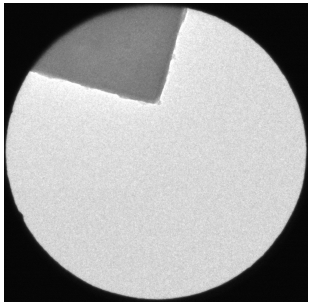

TEM image of corner cube

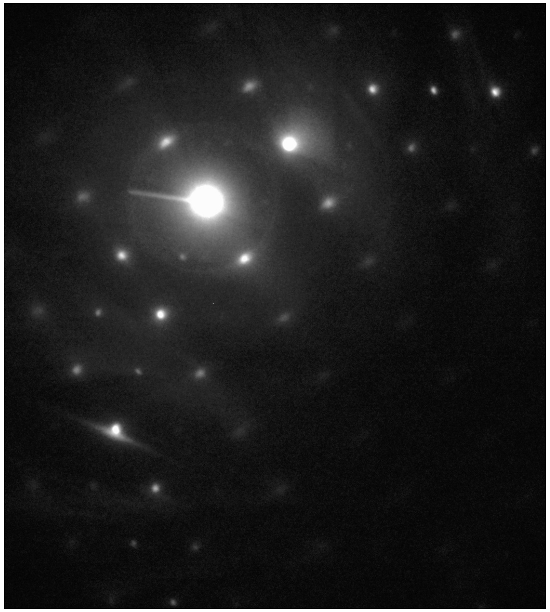

Diffraction pattern of the 110 plane

Diffraction pattern of the 100 plane
in rock salt FCC of PbTe
(TEM image of the investigated area – corner cube)

Material Characterization

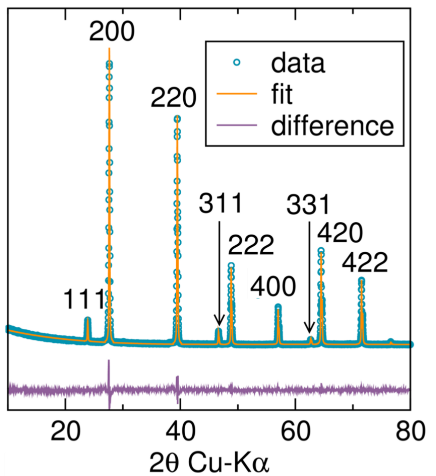

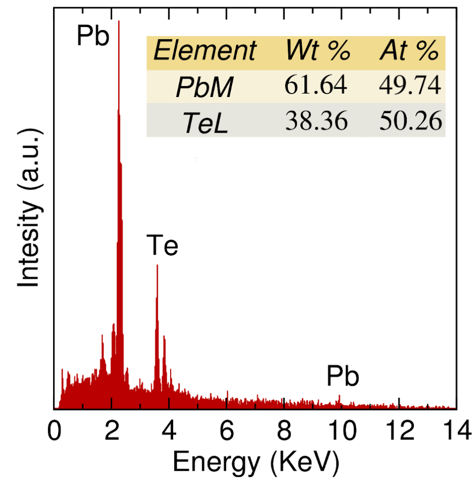

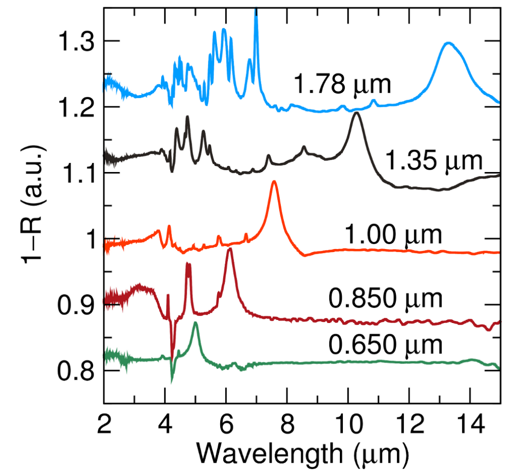

Diffraction pattern of the 100 plane
in rock salt FCC of PbTe (TEM image of the investigated area – corner cube